

Stabilized low-order finite element approximation for linear three-field poroelasticity

Lorenz Berger¹, Rafel Bordas¹, David Kay¹, and Simon Tavenier²

¹Department of Computer Science, University of Oxford

²Department of Mathematics, Colorado State University

November 12, 2018

Abstract

A stabilized conforming finite element method for the three-field (displacement, fluid flux and pressure) poroelasticity problem is presented. We use the lowest possible approximation order: piecewise constant approximation for the pressure, and piecewise linear continuous elements for the displacements and fluid flux. By applying a local pressure jump stabilization term to the mass conservation equation we avoid pressure oscillations and importantly, the discretization leads to a symmetric linear system. For the fully discretized problem we prove existence and uniqueness, an energy estimate and an optimal a-priori error estimate, including an error estimate for the fluid flux in its natural $Hdiv$ norm. Numerical experiments in 2D and 3D illustrate the convergence of the method, show the effectiveness of the method to overcome spurious pressure oscillations, and evaluate the added mass effect of the stabilization term. poroelasticity; stabilized mixed finite elements; well-posedness; a-priori error estimates.

1 Introduction

Poroelasticity is a simplified mixture theory in which a complex fluid-structure interaction problem is approximated by a superposition of both solid and fluid components using averaging techniques. In this work we assume small deformations allowing us to significantly simplify the equations. A detailed discussion and derivation of the general equations can be found in Coussy [2004].

Biot's poroelastic theory has been used in various geomechanical applications ranging from reservoir engineering [Phillips and Wheeler, 2007a] to modelling earthquake fault zones [White and Borja, 2008]. More recently, fully saturated incompressible poroelastic models, often derived using the theory of mixtures [Boer, 2005], have been used for modelling biological tissues. For example, modelling lung parenchyma [Kowalczyk, 1993], protein based hydrogels embedded within cells [Galie et al., 2011], perfusion of blood flow in the beating myocardium [Chapelle et al., 2010; Cookson et al., 2012], the modelling of brain oedema [Li et al., 2010] and hydrocephalus [Wirth and Sobey, 2006], along with the modelling of interstitial fluid and tissue in articular cartilage and intervertebral discs [Galbusera et al., 2011; Holmes and Mow, 1990; Mow et al., 1980]. In this work, we focus on the application of modelling biological tissues, and will therefore restrict the equations to the fully saturated incompressible case. By doing so we minimize complications yet still retain all the numerical difficulties associated with solving the full Biot model, some of which are discussed next.

After many decades of research there remain numerous challenges associated with the numerical solution of the poroelastic equations. When using the finite element method the main challenge is to ensure stability and convergence of the method and prevent numerical instabilities that often manifest themselves in the form of oscillations in the pressure. It has been suggested that this problem is caused by the saddle point structure in the coupled equations resulting in a violation of the famous Ladyzhenskaya-Babuska-Brezzi (LBB) condition [Haga et al., 2012], which highlights the need for a stable combination of mixed finite elements. Another numerical challenge in practical 3D applications is the algebraic system arising from the finite element discretisation. This can lead to a very large matrix system that has many unknowns and is severely ill-conditioned, making it difficult to solve using standard iterative based solvers. Therefore low-order finite element methods that allow for efficient preconditioning are preferred [Ferronato et al., 2010; White and Borja, 2011].

The equations are often solved in a reduced displacement and pressure formulation, from which the fluid flux can then be recovered [Murad and Loula, 1994; White and Borja, 2008]. Murad and Loula [1994] have analysed the stability and convergence of this reduced displacement pressure (\mathbf{u}/p) formulation and were able to show error bounds for inf-sup stable combinations of finite element spaces (e.g. Taylor-Hood elements). In this paper we will keep the fluid flux variable resulting in a three-field, displacement, fluid flux, and pressure formulation. Keeping the fluid flux as a primary variable has the following advantages:

- It avoids the calculation of the fluid flux in post-processing.
- Physically meaningful boundary conditions can be applied at the interface when modelling the interaction between a fluid and a poroelastic structure [Badia et al., 2009].
- It allows for greater accuracy in the fluid velocity field. This can be of interest whenever a consolidation model is coupled with an advection diffusion equation, e.g. to account for thermal effects, contaminant transport or the transport of nutrients or drugs within a porous tissue.
- It allows for an easy extension of the fluid model from a Darcy to a Brinkman flow model, for which there are numerous applications in modelling biological tissues [Khaled and Vafai, 2003].

Phillips and Wheeler [2007a,b], have proved error estimates for solving the three-field formulation problem using continuous piecewise linear approximations for displacements and mixed low-order Raviart Thomas elements for the fluid flux and pressure variables. In Li and Li [2012], a discontinuous method and in Yi [2013] a nonconforming three-field method is analysed. These papers are motivated by the need for a method that is able to overcome pressure oscillations [see, Phillips and Wheeler, 2009] experienced by the method in Phillips and Wheeler [2007a,b]. In addition to these monolithic approaches there has been considerable work on operating splitting (iterative) approaches for solving the poroelastic equations [Feng and He, 2010; Kim et al., 2011; Wheeler and Gai, 2007]. Although these methods are often able to take advantage of existing elasticity and fluid finite element software, and result in solving a smaller system of equations, these schemes are often only conditionally stable, and their accuracy is complicated by the exchange of information between the components [see, Carey et al., 2013]. To ensure that the method is unconditionally stable monolithic approaches are often preferred. The method proposed in this work is monolithic, and will therefore retain the advantage of being unconditionally stable.

To satisfy the LBB condition numerous stabilization techniques for finite element methods have already been proposed, most extensively for the model equations of Stokes and Darcy flow, which despite their simplicity retain all the difficulties of a saddle point problem. A good introduc-

tion on stabilization techniques for the Stokes problem can be found in chapter 5 of Elman et al. [2005]. For a comparison of low-order stabilization techniques for the Darcy problem we refer to Bochev and Dohrmann [2006]. Most stabilized methods lead to a modified variational formulation in which an additional term is added to the mass balance equation, modifying the incompressibility constraint in such a way that stability of the mixed formulation is increased, while still maintaining optimal convergence of the method. These stabilization techniques are of great interest to us since solving the three-field poroelasticity problem is essentially equivalent to coupling the Stokes equations (elasticity of the porous mixture) with the Darcy equations (fluid flow through pores), with a modified incompressibility constraint that combines the divergence of the displacement velocity and the fluid flux. In this work we will use the local pressure jump stabilization method that has already successfully been used for solving the Stokes and Darcy equations independently or coupled via an interface [see, Burman and Hansbo, 2007]. Further, this approach provides the natural H^1 stability for the displacements and $H\text{div}$ stability for the flux. This mixed scheme uses the lowest possible approximation order, piecewise constant approximation for the pressure and piecewise linear continuous elements for the displacement and fluid flux. A motivation for using piecewise constant pressure elements is that in practical scenarios the domain often has large permeability contrasts, and the solution may then contain steep pressure gradients. In this situation continuous pressure elements often struggle to capture the steep gradient at the interface between the high-permeable and low-permeable region, and as a result overshoot the true solution. By using a low-order piecewise constant (discontinuous) approximation for the pressure we can approximate these steep pressure gradients reliably, and avoid localized oscillations in the pressure [White and Borja, 2008]. There are also other practical advantages from using low-order interpolation elements, such as obtaining a linear system that is smaller relative to accuracy and has less bandwidth, and ease of implementation and discretization of geometrically complicated domains. The resulting linear system is also symmetric and has a nice block structure that is well suited for effective preconditioning.

The rest of this paper is organized as follows: in section 1.1, we describe the model equations; in section 2 we present the continuous weak formulation of the model; in section 3 we introduce the fully-discrete model, prove existence and uniqueness at each time step, and give an energy estimate over time. We then derive an optimal order a-priori error estimate in section 4. Finally in section 5, we present some numerical experiments that verify our theoretical findings in 2D and 3D, test the robustness of the method, and show that it is able to overcome pressure oscillations.

1.1 The model

The governing equations of the Biot model, with the displacement \mathbf{u} , fluid flux \mathbf{z} , and pressure p as primary variables are summarized below:

$$-\nabla \cdot \sigma = \mathbf{f} \quad \text{in } \Omega, \quad (1a)$$

$$\kappa^{-1} \mathbf{z} + \nabla p = \mathbf{b} \quad \text{in } \Omega, \quad (1b)$$

$$\nabla \cdot \mathbf{z} + \frac{\partial}{\partial t}(\alpha \nabla \cdot \mathbf{u} + c_0 p) = g \quad \text{in } \Omega, \quad (1c)$$

$$\mathbf{u}(t) = \mathbf{u}_D \quad \text{on } \Gamma_d, \quad (1d)$$

$$\sigma(t) \mathbf{n} = \mathbf{t}_N \quad \text{on } \Gamma_t, \quad (1e)$$

$$p(t) = p_D \quad \text{on } \Gamma_p, \quad (1f)$$

$$\mathbf{z}(t) \cdot \mathbf{n} = q_D \quad \text{on } \Gamma_f, \quad (1g)$$

$$\mathbf{u}(0) = \mathbf{u}^0, \quad p(0) = p^0, \quad \text{in } \Omega, \quad (1h)$$

where σ is the total stress tensor given by $\sigma = \lambda \text{tr}(\epsilon(\mathbf{u})) \mathbf{I} + 2\mu_s \epsilon(\mathbf{u}) - \alpha p \mathbf{I}$, with the linear strain tensor defined as $\epsilon(\mathbf{u}) = \frac{1}{2} (\nabla \mathbf{u} + (\nabla \mathbf{u})^T)$, g is the fluid source term, \mathbf{f} is the body force on the mixture, and \mathbf{b} is the body force on the fluid. Here Ω is a bounded domain in \mathbb{R}^2 or \mathbb{R}^3 , and for the purpose of defining boundary conditions, $\partial\Omega = \Gamma_d + \Gamma_t$ for displacement and stress boundary conditions and $\partial\Omega = \Gamma_p + \Gamma_f$ for pressure and flux boundary conditions, with outward pointing unit normal \mathbf{n} . The parameters along with a description are given in Table 1.

Parameter	
Lamé's first parameter	λ ,
Lamé's second parameter (shear modulus)	μ_s ,
Dynamic permeability tensor	κ ,
Solid skeleton density	ρ_s
Fluid density	ρ_f
Biot-Willis constant	α ,
Constrained specific storage coefficient	c_0 .

Table 1: Poroelasticity parameters.

We have also set $\kappa = \mu_f^{-1} \mathbf{k}$, where μ_f and \mathbf{k} are the fluid viscosity and the permeability tensor, respectively. A derivation and more detailed explanation of these equations can be found in Phillips and Wheeler [2007a] and Showalter [2000]. In this work we will consider a simplification of the full Biot model (1), by setting $\alpha = 1$ and $c_0 = 0$. This yields the following fully saturated

and incompressible model:

$$-(\lambda + \mu_s)\nabla(\nabla \cdot \mathbf{u}) - \mu_s \nabla^2 \mathbf{u} + \nabla p = \mathbf{f} \quad \text{in } \Omega, \quad (2a)$$

$$\kappa^{-1} \mathbf{z} + \nabla p = \mathbf{b} \quad \text{in } \Omega, \quad (2b)$$

$$\nabla \cdot (\mathbf{u}_t + \mathbf{z}) = g \quad \text{in } \Omega, \quad (2c)$$

$$\mathbf{u}(t) = \mathbf{u}_D \quad \text{on } \Gamma_d, \quad (2d)$$

$$\sigma(t) \mathbf{n} = \mathbf{t}_N \quad \text{on } \Gamma_t, \quad (2e)$$

$$p(t) = p_D \quad \text{on } \Gamma_p, \quad (2f)$$

$$\mathbf{z}(t) \cdot \mathbf{n} = q_D \quad \text{on } \Gamma_f, \quad (2g)$$

$$\mathbf{u}(0) = \mathbf{u}^0 \quad \text{in } \Omega, \quad (2h)$$

The extension of the theoretical results presented in this work to the full Biot equations (1), with $\alpha \in \mathbb{R}_{>0}$ and $c_0 \in \mathbb{R}_{>0}$ is straightforward. In the analysis, the constant α would just get absorbed by a general constant C . When $c_0 > 0$, an additional pressure term is introduced into the mass conservation equation. Since this term is coercive, it can only improve the stability of the system.

2 Weak formulation

Before presenting the weak formulation of (2), we first need to introduce some notation and bilinear forms. We introduce the space $L_0^2(\Omega) := \{q \in L^2(\Omega) : \int_\Omega q \, dx = 0\}$, and define

$$\mathcal{L}(\Omega) := \begin{cases} L^2(\Omega) & \text{if } \Gamma_t \cup \Gamma_p \neq \emptyset \\ L_0^2(\Omega) & \text{if } \Gamma_t \cup \Gamma_p = \emptyset \end{cases}$$

We let $\mathbf{W}^E = \{\mathbf{u} \in H^1(\Omega, \mathbb{R}^d) : \mathbf{u} = \mathbf{u}_D \text{ on } \Gamma_d\}$, $\mathbf{W}^D = \{\mathbf{z} \in H_{div}(\Omega, \mathbb{R}^d) : \mathbf{z} \cdot \mathbf{n} = q_D \text{ on } \Gamma_f\}$. We also define the mixed solution space $\mathcal{W}^X = \{\mathbf{W}^E \times \mathbf{W}^D \times \mathcal{L}(\Omega)\}$. For the test functions we define the spaces $\mathbf{W}_0^E = \{\mathbf{v} \in H^1(\Omega, \mathbb{R}^d) : \mathbf{v} = 0 \text{ on } \Gamma_d\}$, $\mathbf{W}_0^D = \{\mathbf{w} \in H_{div}(\Omega, \mathbb{R}^d) : \mathbf{w} \cdot \mathbf{n} = 0 \text{ on } \Gamma_f\}$, and $\mathcal{V}^X = \{\mathbf{W}_0^E \times \mathbf{W}_0^D \times \mathcal{L}(\Omega)\}$. With $\mathbf{u} \in \mathbf{W}^E$ and $\mathbf{v} \in \mathbf{W}_0^E$, we define the bilinear form

$$a(\mathbf{u}, \mathbf{v}) = \int_\Omega 2\mu_s(\epsilon(\mathbf{u}) : \epsilon(\mathbf{v})) + \lambda(\nabla \cdot \mathbf{u})(\nabla \cdot \mathbf{v}) \, dx,$$

which corresponds to the elasticity part of the mixture momentum equation (2a). This bilinear form is continuous such that

$$a(\mathbf{u}, \mathbf{v}) \leq C_c \|\mathbf{u}\|_{1,\Omega} \|\mathbf{v}\|_{1,\Omega} \quad \forall \mathbf{u}, \mathbf{v} \in H^1(\Omega, \mathbb{R}^d). \quad (3)$$

In addition, using Korn's inequality [see 11.2.22 in Brenner and Scott, 2008], and $\int_\Omega \lambda(\nabla \cdot \mathbf{v})(\nabla \cdot \mathbf{v}) \geq 0$ we have

$$\|\mathbf{v}\|_{a,\Omega}^2 = a(\mathbf{v}, \mathbf{v}) \geq 2\mu_s \|\epsilon(\mathbf{v})\|_{0,\Omega}^2 \geq C_k \|\mathbf{v}_h\|_{1,\Omega}^2 \quad \forall \mathbf{v} \in \mathbf{W}_0^E. \quad (4)$$

We also have

$$\lambda_{min}^{-1} \|\mathbf{w}\|_{0,\Omega}^2 \geq (\kappa^{-1} \mathbf{w}, \mathbf{w}) \geq \lambda_{max}^{-1} \|\mathbf{w}\|_{0,\Omega}^2 \quad \forall \mathbf{w} \in \mathbf{W}_0^D, \quad (5)$$

since κ is assumed to be a symmetric and positive definite tensor, there exists $\lambda_{min}, \lambda_{max} > 0$ such that $\forall \mathbf{x} \in \Omega$, $\lambda_{min} \|\eta\|_{0,\Omega} \leq \eta^t \kappa(\mathbf{x}) \eta \leq \lambda_{max} \|\eta\|_{0,\Omega} \quad \forall \eta \in \mathbb{R}^d$, by the boundedness of κ [see, Phillips and Wheeler, 2007a].

2.1 Continuous weak formulation

We now multiply the strong form of the problem (2) by test functions $(\mathbf{v}, \mathbf{w}, q) \in \mathcal{V}^X$ and integrate to yield the continuous weak problem, which is to find $\mathbf{u}(x, t) \in \mathbf{W}^E$, $\mathbf{z}(x, t) \in \mathbf{W}^D$, and $p(x, t) \in \mathcal{L}(\Omega)$ for any time $t \in [0, T]$ such that:

$$a(\mathbf{u}, \mathbf{v}) - (p, \nabla \cdot \mathbf{v}) = (\mathbf{f}, \mathbf{v}) + (\mathbf{t}_N, \mathbf{v})_{\Gamma_t} \quad \forall \mathbf{v} \in \mathbf{W}_0^E, \quad (6a)$$

$$(\kappa^{-1} \mathbf{z}, \mathbf{w}) - (p, \nabla \cdot \mathbf{w}) = (\mathbf{b}, \mathbf{w}) - (p_D, \mathbf{w} \cdot \mathbf{n})_{\Gamma_p} \quad \forall \mathbf{w} \in \mathbf{W}_0^D, \quad (6b)$$

$$(\nabla \cdot \mathbf{u}_t, q) + (\nabla \cdot \mathbf{z}, q) = (g, q) \quad \forall q \in \mathcal{L}(\Omega). \quad (6c)$$

We will assume the following regularity requirements on the data:

$$\mathbf{f} \in C^1([0, T] : (H^{-1}(\Omega))^d), \quad (7a)$$

$$\mathbf{b} \in C^1([0, T] : (H_{div}^{-1}(\Omega))^d), \quad (7b)$$

$$g \in C^0([0, T] : (L^2(\Omega))^d), \quad (7c)$$

$$\mathbf{u}_D \in C^1([0, T] : H^{1/2}(\Gamma_d)), \quad (7d)$$

$$\mathbf{t}_N \in C^1([0, T] : H^{-1/2}(\Gamma_t)), \quad (7e)$$

$$q_D \in C^0([0, T] : TrW), \quad (7f)$$

$$p_D \in C^0([0, T] : L^2(\Gamma_p)), \quad (7g)$$

where $TrW := \{\mathbf{w} \cdot \mathbf{n}|_{\Gamma_f} : \mathbf{w} \in (H_{div}(\Omega))^d\}$. For the initial conditions we require that

$$\mathbf{u}^0 \in (H^1(\Omega))^d, \quad \mathbf{z}^0 \in (H_{div}(\Omega))^d, \quad p^0 \in \mathcal{L}(\Omega). \quad (8)$$

The well-posedness of the continuous field formulation has been proven by Showalter [2000]. Lipnikov [2002] proves well-posedness for the continuous three-field formulation (6). In this work we also establish the well-posedness of (6) as a result of the energy estimates proven in section 3.2, see remark 1.

3 Fully-discrete model

We begin with some standard finite element notation. Let $K = \{E_1, E_2, \dots, E_{M_h}\}$ be a subdivision of Ω , where E_j is a d -simplex. Let $h_j = \text{diam}(E_j)$ and set $h = \max \{h_j : j = 1, \dots, M_h\}$. The mixed finite element space defined on K is given as $\mathcal{W}_h^X = (\mathbf{W}_h^E \times \mathbf{W}_h^D \times Q_h) \subset (\mathbf{W}^E \times \mathbf{W}^D \times \mathcal{L}(\Omega))$, similarly for the test function we let $\mathcal{V}_h^X = (\mathbf{W}_{h0}^E \times \mathbf{W}_{h0}^D \times Q_h) \subset (\mathbf{W}_0^E \times \mathbf{W}_0^D \times \mathcal{L}(\Omega))$. We will now give a stabilized conforming mixed finite element method for discretization of (6). To discretize the time derivative we use the fully implicit backward Euler scheme, which we will denote using the shorthand $v_{\delta t}^n := \frac{v^n - v^{n-1}}{\Delta t}$. Let \mathbf{u}_h denote the approximate displacement solution over all time steps, such that $\mathbf{u}_h = [\mathbf{u}_h^0, \mathbf{u}_h^1, \dots, \mathbf{u}_h^N]$, and similarly for the other variables. We also add the pressure jump term $J(p_{\delta t, h}, q_h)$ to stabilize the system. The fully discretized weak problem is now to find $\mathbf{u}_h^n \in \mathbf{W}_h^E$, $\mathbf{z}_h^n \in \mathbf{W}_h^D$ and $p_h^n \in Q_h$ such that:

$$a(\mathbf{u}_h^n, \mathbf{v}_h) - (p_h^n, \nabla \cdot \mathbf{v}_h) = (\mathbf{f}^n, \mathbf{v}_h) + (\mathbf{t}_N, \mathbf{v}_h)_{\Gamma_t} \quad \forall \mathbf{v}_h \in \mathbf{W}_{h0}^E, \quad (9a)$$

$$(\kappa^{-1} \mathbf{z}_h^n, \mathbf{w}_h) - (p_h^n, \nabla \cdot \mathbf{w}_h) = (\mathbf{b}^n, \mathbf{w}_h) - (p_D, \mathbf{w}_h \cdot \mathbf{n})_{\Gamma_p} \quad \forall \mathbf{w}_h \in \mathbf{W}_{h0}^D, \quad (9b)$$

$$(\nabla \cdot \mathbf{u}_{\delta t, h}^n, q_h) + (q_h, \nabla \cdot \mathbf{z}_h^n) + J(p_{\delta t, h}, q_h) = (g^n, q_h) \quad \forall q_h \in Q_h. \quad (9c)$$

We also choose the following initial conditions

$$a(\mathbf{u}_h^0, \mathbf{v}) = a(\mathbf{u}^0, \mathbf{v}) \quad \forall \mathbf{v}_h \in \mathbf{W}_{h0}^E, \quad (10a)$$

$$(p_h^0, q_h) = (p^0, q_h) \quad \forall q_h \in Q_h. \quad (10b)$$

The stabilization term is given by, see Burman and Hansbo [2007],

$$J(p, q) = \delta \sum_K \int_{\partial K \setminus \partial \Omega} h_{\partial K} [p][q] \, ds.$$

Here δ is a penalty parameter that is independent of h and Δt . We will see in the numerical results, section 5 that the convergence is not sensitive to δ . The set of all elements is denoted by K , $h_{\partial K}$ denotes the size of an element edge in 2D or face in 3D, and $[\cdot]$ is the jump across an edge. As an example consider $[p_h]$, the jump operator on the piecewise constant pressure. The scalar jump in pressure $[p_h]$ across an edge or face adjoining the interior element T and the exterior S element is defined as $[p_h] := (p_h|_T - p_h|_S)$. The stabilization term also gives rise to the semi-norm $\|q\|_{J,\Omega} = J(q, q)^{1/2}$. Throughout this work, we will let C denote a generic positive constant, whose value may change from instance to instance, but is independent of any mesh parameters. We now have the following bound for the stabilization term

$$J(q_h, q_h) \leq \|q_h\|_{J,\Omega} \|q_h\|_{J,\Omega} \leq \left(C \|q_h\|_{0,\Omega}^2 + hC \|q_h\|_{1,\Omega} \|q_h\|_{0,\Omega} \right) \leq \|q_h\|_{0,\Omega}^2. \quad (11)$$

The first inequality above comes from an application of the Cauchy-Schwarz inequality, the second step is possible due to the the following trace inequality from lemma 3.1 in Verfürth [1998], which can be written as

$$\|\mathbf{v} \cdot \mathbf{n}\|_{0,\partial K}^2 \leq C \|\mathbf{v}\|_{0,K} (h^{-1} \|\mathbf{v}\|_{0,K} + \|\mathbf{v}\|_{1,K}), \quad (12)$$

and in the final step we have used the inverse estimate $\|v\|_{1,\Omega} \leq \frac{C}{h} \|v\|_{0,\Omega}$.

3.1 Existence and uniqueness of the fully-discrete model at a time step

The well-posedness of the the fully-discretized system (3) with $\delta = 0$ and the additional term arising from $c_0 > 0$ is shown by Phillips and Wheeler [2007b]. Lipnikov [2002] shows the more general case for $c_0 \geq 0$. As the permeability tends to zero and the porous mixture becomes impermeable, the three-field linear poroelasticity tends to a mixed linear elasticity problem. The choice of the mixed finite element space then also needs to be stable for the mixed linear elasticity problem [see, Haga et al., 2012]. However the discretization methods presented in Phillips and Wheeler [2007b] and Lipnikov [2002] both use piecewise linear approximations for displacements and mixed low-order Raviart Thomas elements for the fluid flux and pressure variables. It is well known that a piecewise linear approximations for displacements and piecewise constant approximation for the pressure is not a stable element combination for the mixed linear elasticity problem. We hypothesise that this is why the method presented by Phillips and Wheeler [2007b] experiences numerical instabilities, as is shown in Phillips and Wheeler [2008] and Phillips and Wheeler [2009]. Our proposed stabilized method is stable for both the Darcy problem (as the elasticity coefficients tend to infinity) and the mixed linear elasticity problem (as the permeability tends to zero), and therefore is stable for all permeabilities.

Combining the fully discrete balance equations (9a), (9b) and (9c), and multiplying (9b) and (9c) by Δt we get the following

$$B_h^n[(\mathbf{u}_h, \mathbf{z}_h, p_h), (\mathbf{v}_h, \mathbf{w}_h, q_h)] = (\mathbf{f}^n, \mathbf{v}_h) + (\mathbf{t}_N, \mathbf{v}_h)_{\Gamma_t} + \Delta t(\mathbf{b}^n, \mathbf{w}_h) - \Delta t(p_D, \mathbf{w}_h \cdot \mathbf{n})_{\Gamma_p} + \Delta t(g^n, q_h) + (\nabla \cdot \mathbf{u}_h^{n-1}, q_h) + J(p_h^{n-1}, q_h) \quad \forall (\mathbf{v}_h, \mathbf{w}_h, q_h) \in \mathcal{W}_h^X, \quad (13)$$

where

$$B_h^n[(\mathbf{u}_h, \mathbf{z}_h, p_h), (\mathbf{v}_h, \mathbf{w}_h, q_h)] = a(\mathbf{u}_h^n, \mathbf{v}_h) + \Delta t(\kappa^{-1} \mathbf{z}_h^n, \mathbf{w}_h) - (p_h^n, \nabla \cdot \mathbf{v}_h) - \Delta t(p_h^n, \nabla \cdot \mathbf{w}_h) + (\nabla \cdot \mathbf{u}_h^n, q_h) + \Delta t(\nabla \cdot \mathbf{z}_h^n, q_h) + J(p_h^n, q_h). \quad (14)$$

We also define the following triple-norm:

$$|||(\mathbf{u}_h^n, \mathbf{z}_h^n, p_h^n)|||_{\mathcal{W}_h^X} = \|\mathbf{u}_h^n\|_{1,\Omega} + \Delta t \|\nabla \cdot \mathbf{z}_h^n\|_{0,\Omega} + \Delta t^{1/2} \|\mathbf{z}_h^n\|_{0,\Omega} + \|p_h^n\|_{0,\Omega} + \|p_h^n\|_{J,\Omega}, \quad (15)$$

and for the test functions the triple-norm:

$$|||(\mathbf{v}_h, \mathbf{w}_h, q_h)|||_{\mathcal{V}_h^X} = \|\mathbf{v}_h\|_{1,\Omega} + \Delta t \|\nabla \cdot \mathbf{w}_h\|_{0,\Omega} + \Delta t^{1/2} \|\mathbf{w}_h\|_{0,\Omega} + \|q_h\|_{0,\Omega} + \|q_h\|_{J,\Omega}. \quad (16)$$

Note that these triple-norms satisfies the required continuity property

$$|B_h^n[(\mathbf{u}_h, \mathbf{z}_h, p_h), (\mathbf{v}_h, \mathbf{w}_h, q_h)]| \leq C |||(\mathbf{u}_h^n, \mathbf{z}_h^n, p_h^n)|||_{\mathcal{W}_h^X} |||(\mathbf{v}_h, \mathbf{w}_h, q_h)|||_{\mathcal{V}_h^X}.$$

We will now apply Babuska's theory [Babuska, 1971] to show well-posedness (existence and uniqueness) of this discretized system at a particular time step. This requires us to prove a discrete inf-sup type result (Theorem 3.1) for the combined bilinear form (14). This will ensure that the linear system resulting from the discretization has full rank.

Theorem 3.1. *Let $\gamma > 0$ be a constant independent of any mesh parameters. Then the finite element formulation (9) satisfies the following discrete inf-sup condition*

$$\gamma |||(\mathbf{u}_h^n, \mathbf{z}_h^n, p_h^n)|||_{\mathcal{W}_h^X} \leq \sup_{(\mathbf{v}_h, \mathbf{w}_h, q_h) \in \mathcal{V}_h^X} \frac{B_h^n[(\mathbf{u}_h, \mathbf{z}_h, p_h), (\mathbf{v}_h, \mathbf{w}_h, q_h)]}{|||(\mathbf{v}_h, \mathbf{w}_h, q_h)|||_{\mathcal{V}_h^X}} \quad \forall (\mathbf{u}_h, \mathbf{z}_h, p_h) \in \mathcal{W}_h^X. \quad (17)$$

The following proof follows ideas presented by Burman and Hansbo [2007].

Proof.

Step 1, bounding $\|\mathbf{u}_h^n\|_{1,\Omega}$, $\Delta t^{1/2} \|\mathbf{z}_h^n\|_{0,\Omega}$, and $\|p_h^n\|_{J,\Omega}$.

Choose $(\mathbf{v}_h, \mathbf{w}_h, q_h) = (\mathbf{u}_h^n, \mathbf{z}_h^n, p_h^n)$, then using (4) and (5), we obtain,

$$B_h^n[(\mathbf{u}_h, \mathbf{z}_h, p_h), (\mathbf{u}_h, \mathbf{z}_h, p_h)] = a(\mathbf{u}_h^n, \mathbf{u}_h^n) + \Delta t(\kappa^{-1} \mathbf{z}_h^n, \mathbf{z}_h^n) + J(p_h^n, p_h^n) \geq C_k \|\mathbf{u}_h^n\|_{1,\Omega}^2 + \lambda_{max}^{-1} \Delta t \|\mathbf{z}_h^n\|_{0,\Omega}^2 + \|p_h^n\|_{J,\Omega}^2. \quad (18)$$

Step 2, bounding $\|p_h^n\|_{0,\Omega}$.

Due to the surjectivity of the divergence operator there exists a function $\mathbf{v}_p \in [H_0^1]^d$ such that $\nabla \cdot \mathbf{v}_p = -p_h^n$ and $\|\mathbf{v}_p\|_{1,\Omega} \leq c \|p_h^n\|_{0,\Omega}$, with $p_h^n \in Q_h$. Let $\pi_h \mathbf{v}_p$ denote the projection of $\mathbf{v}_p \in$

$[H_0^1]^d$ onto \mathbf{W}_{h0}^E . This projection is known as the Scott-Zhang projection [see section 4.8 in Brenner and Scott, 2008], and will allow us to obtain stability of the pressure and avoid spurious pressure oscillations. The discrepancy between the projection and its continuous counterpart will eventually be made up by the stabilization term. We assume that the projection is stable such that

$$\|\pi_h \mathbf{v}_p\|_{1,\Omega} \leq \hat{c} \|p_h^n\|_{0,\Omega}, \quad (19)$$

which also gives

$$\|\pi_h \mathbf{v}_p\|_{0,\Omega} \leq \hat{c} \|p_h^n\|_{0,\Omega}. \quad (20)$$

Choose $(\mathbf{v}_h, \mathbf{w}_h, q_h) = (\pi_h \mathbf{v}_p, 0, 0)$ and add $0 = \|p_h^n\|_{0,\Omega}^2 + (p_h^n, \nabla \cdot \mathbf{v}_p)$ to obtain

$$B_h^n[(\mathbf{u}_h, \mathbf{z}_h, p_h), (\pi_h \mathbf{v}_p, 0, 0)] = a(\mathbf{u}_h^n, \pi_h \mathbf{v}_p) + \|p_h^n\|_{0,\Omega}^2 + (p_h^n, \nabla \cdot (\mathbf{v}_p - \pi_h \mathbf{v}_p)). \quad (21)$$

Focusing on the third term in (21) only, we apply the divergence theorem and split the integral over local elements to get

$$(p_h^n, \nabla \cdot (\mathbf{v}_p - \pi_h \mathbf{v}_p)) = \sum_K \int_{\partial K} p_h^n \cdot (\mathbf{v}_p - \pi_h \mathbf{v}_p) \cdot \mathbf{n} \, ds = \sum_K \frac{1}{2} \int_{\partial K} [p_h^n] \cdot (\mathbf{v}_p - \pi_h \mathbf{v}_p) \cdot \mathbf{n} \, ds.$$

We thus have

$$B_h^n[(\mathbf{u}_h, \mathbf{z}_h, p_h), (\pi_h \mathbf{v}_p, 0, 0)] = \|p_h^n\|_{0,\Omega}^2 + a(\mathbf{u}_h^n, \pi_h \mathbf{v}_p) + \sum_K \frac{1}{2} \int_{\partial K} [p_h^n] \cdot (\mathbf{v}_p - \pi_h \mathbf{v}_p) \cdot \mathbf{n} \, ds.$$

Now first applying the Cauchy-Schwarz inequality and (3) on the right hand side we get

$$\begin{aligned} B_h^n[(\mathbf{u}_h, \mathbf{z}_h, p_h), (\pi_h \mathbf{v}_p, 0, 0)] &\geq \|p_h^n\|_{0,\Omega}^2 - C_c \|\mathbf{u}_h^n\|_{1,\Omega} \|\pi_h \mathbf{v}_p\|_{1,\Omega} \\ &\quad - \sum_K \frac{1}{2} \left(\int_{\partial K} \left(h^{1/2} [p_h^n] \right)^2 \, ds \right)^{1/2} \cdot \left(\int_{\partial K} \left(h^{-1/2} (\mathbf{v}_p - \pi_h \mathbf{v}_p) \cdot \mathbf{n} \right)^2 \, ds \right)^{1/2}. \end{aligned}$$

Now apply Young's inequality (i.e., for $a, b \geq 0, a \geq 0, ab \leq \frac{1}{2\epsilon} a^2 + \frac{\epsilon}{2} b^2$), and the bound of the projection (19), to obtain

$$\begin{aligned} B_h^n[(\mathbf{u}_h, \mathbf{z}_h, p_h), (\pi_h \mathbf{v}_p, 0, 0)] &\geq \|p_h^n\|_{0,\Omega}^2 - \frac{C_c^2}{2\epsilon} \|\mathbf{u}_h^n\|_{1,\Omega}^2 - \frac{\epsilon \hat{c}}{2} \|p_h^n\|_{0,\Omega}^2 \\ &\quad - \frac{1}{4\epsilon} J(p_h^n, p_h^n) - \frac{\epsilon}{4} \sum_K \int_{\partial K} h^{-1} |(\mathbf{v}_p - \pi_h \mathbf{v}_p) \cdot \mathbf{n}|^2 \, ds. \end{aligned}$$

Hence,

$$\begin{aligned} B_h^n[(\mathbf{u}_h, \mathbf{z}_h, p_h), (\pi_h \mathbf{v}_p, 0, 0)] &\geq -\frac{C_c^2}{2\epsilon} \|\mathbf{u}_h^n\|_{1,\Omega}^2 + (1 - \frac{\epsilon \hat{c}}{2}) \|p_h^n\|_{0,\Omega}^2 \\ &\quad - \frac{1}{4\epsilon} J(p_h^n, p_h^n) - \frac{\epsilon}{4} \sum_K \int_{\partial K} h^{-1} |(\mathbf{v}_p - \pi_h \mathbf{v}_p) \cdot \mathbf{n}|^2 \, ds. \end{aligned}$$

Recall the trace inequality from lemma 3.1 in Verfürth [1998], which can be written as

$$\|\mathbf{v} \cdot \mathbf{n}\|_{0,\partial K}^2 \leq C \|\mathbf{v}\|_{0,K} (h^{-1} \|\mathbf{v}\|_{0,K} + \|\mathbf{v}\|_{1,K}). \quad (22)$$

Substituting $\mathbf{v} = (\mathbf{v}_p - \pi_h \mathbf{v}_p)$ in (22) and noting that $\|\mathbf{v}_p - \pi_h \mathbf{v}_p\|_{0,K} \leq Ch\|\mathbf{v}_p\|_{1,K}$ we arrive at

$$\|(\mathbf{v}_p - \pi_h \mathbf{v}_p) \cdot \mathbf{n}\|_{0,\partial K}^2 \leq Ch\|\mathbf{v}_p\|_{1,K}^2.$$

Taking into account $\|\mathbf{v}_p\|_{1,\Omega} \leq c\|p_h^n\|_{0,\Omega}$, we may write

$$\sum_K \int_{\partial K} h^{-1} |(\mathbf{v}_p - \pi_h \mathbf{v}_p) \cdot \mathbf{n}|^2 ds \leq c_t \|p_h^n\|_{0,\Omega}^2,$$

which leads to

$$B_h^n[(\mathbf{u}_h, \mathbf{z}_h, p_h), (\pi_h \mathbf{v}_p, 0, 0)] \geq -\frac{C_c^2}{2\epsilon} \|\mathbf{u}_h^n\|_{1,\Omega}^2 + \left(1 - \left(\hat{c} + \frac{c_t}{2}\right) \frac{\epsilon}{2}\right) \|p_h^n\|_{0,\Omega}^2 - \frac{1}{4\epsilon} \|p_h^n\|_{J,\Omega}^2. \quad (23)$$

Step 3, bounding $\Delta t \|\nabla \cdot \mathbf{z}_h^n\|_{0,\Omega}$.

Choosing $(\mathbf{v}_h, \mathbf{w}_h, q_h) = (0, 0, \Delta t \nabla \cdot \mathbf{z}_h^n)$ yields

$$B_h^n[(\mathbf{u}_h, \mathbf{z}_h, p_h), (0, 0, \Delta t \nabla \cdot \mathbf{z}_h^n)] = (\nabla \cdot \mathbf{u}_h^n, \Delta t \nabla \cdot \mathbf{z}_h^n) + \Delta t^2 \|\nabla \cdot \mathbf{z}_h^n\|_{0,\Omega}^2 + J(p_h^n, \Delta t \nabla \cdot \mathbf{z}_h^n).$$

We bound the first term using the Cauchy-Schwarz inequality followed by Young's inequality such that

$$(\nabla \cdot \mathbf{u}_h^n, \Delta t \nabla \cdot \mathbf{z}_h^n) \leq \frac{C_p}{2\epsilon} \|\mathbf{u}_h^n\|_{1,\Omega}^2 + \frac{\epsilon \Delta t^2}{2} \|\nabla \cdot \mathbf{z}_h^n\|_{0,\Omega}^2.$$

We can also bound the third term as before using the Cauchy-Schwarz inequality followed by Young's inequality such that

$$\begin{aligned} J(p_h^n, \Delta t \nabla \cdot \mathbf{z}_h^n) &\leq \frac{1}{2\epsilon} J(p_h^n, p_h^n) + \frac{\epsilon \Delta t^2}{2} J(\nabla \cdot \mathbf{z}_h^n, \nabla \cdot \mathbf{z}_h^n) \leq \frac{1}{2\epsilon} J(p_h^n, p_h^n) + \epsilon C \Delta t^2 \sum_K \int_{\partial K} |h^{1/2} \nabla \cdot \mathbf{z}_h^n|^2 ds \\ &\leq \frac{1}{2\epsilon} J(p_h^n, p_h^n) + \epsilon c_z \Delta t^2 \|\nabla \cdot \mathbf{z}_h^n\|_{0,\Omega}^2. \end{aligned} \quad (24)$$

Here we have used a scaling argument which relates line and surface integrals and assumes that $\nabla \cdot \mathbf{z}_h^n$ is element-wise constant. The scaling argument, also used in Burman and Hansbo [2007], is that

$C \|h^{1/2} \nabla \cdot \mathbf{z}_h^n\|_{0,\partial K} \leq c_z \|\nabla \cdot \mathbf{z}_h^n\|_{0,K}$. This yields

$$B_h^n[(\mathbf{u}_h, \mathbf{z}_h, p_h), (0, 0, \Delta t \nabla \cdot \mathbf{z}_h^n)] \geq (1 - \epsilon c_z - \frac{\epsilon}{2}) \Delta t^2 \|\nabla \cdot \mathbf{z}_h^n\|_{0,\Omega}^2 - \frac{1}{2\epsilon} \|p_h^n\|_{J,\Omega}^2 - \frac{C_p}{2\epsilon} \|\mathbf{u}_h^n\|_{1,\Omega}^2. \quad (25)$$

Combining all the steps. Finally we can combine (18), (23) and (25) to get control over all the norms by choosing $(\mathbf{v}_h, \mathbf{w}_h, q_h) = (\beta \mathbf{u}_h^n + \pi_h \mathbf{v}_p, \beta \mathbf{z}_h^n, \beta p_h^n + \Delta t \nabla \cdot \mathbf{z}_h^n)$, which yields

$$\begin{aligned} B_h^n[(\mathbf{u}_h, \mathbf{z}_h, p_h), (\beta \mathbf{u}_h^n + \pi_h \mathbf{v}_p, \beta \mathbf{z}_h^n, \beta p_h^n + \Delta t \nabla \cdot \mathbf{z}_h^n)] &\geq \\ &(\beta C_k - \frac{C_c^2 + C_p}{2\epsilon}) \|\mathbf{u}_h^n\|_{1,\Omega}^2 + \beta \lambda_{max}^{-1} \Delta t \|\mathbf{z}_h^n\|_{0,\Omega}^2 + \left(1 - \epsilon c_z - \frac{\epsilon}{2}\right) \Delta t^2 \|\nabla \cdot \mathbf{z}_h^n\|_{0,\Omega}^2 \\ &\quad + \left(1 - \left(\hat{c} + \frac{c_t}{2}\right) \frac{\epsilon}{2}\right) \|p_h^n\|_{0,\Omega}^2 + \left(\beta - \frac{3}{4\epsilon}\right) \|p_h^n\|_{J,\Omega}^2, \end{aligned} \quad (26)$$

where we can choose

$$\beta \geq \max \left[\frac{C_c^2 + C_p}{2\epsilon C_k} + \frac{1 - \bar{C}\epsilon}{C_k}, \lambda_{\max} (1 - \bar{C}\epsilon), \frac{3}{4\epsilon} + 1 - \bar{C}\epsilon \right],$$

with $\bar{C} = \max \left[\frac{\hat{c}}{2} + \frac{c_t}{4}, c_z - \frac{1}{2} \right]$. This yields

$$B_h^n[(\mathbf{u}_h, \mathbf{z}_h, p_h), (\beta \mathbf{u}_h^n + \pi_h \mathbf{v}_p, \beta \mathbf{z}_h^n, \beta p_h^n + \nabla \cdot \mathbf{z}_h^n)] \geq (1 - \bar{C}\epsilon) \|(\mathbf{u}_h^n, \mathbf{z}_h^n, p_h^n)\|_{\mathcal{W}_h^X}^2.$$

To complete the proof we need to take ϵ sufficiently small and show that there exists a constant C such that $\|(\mathbf{u}_h^n, \mathbf{z}_h^n, p_h^n)\|_{\mathcal{W}_h^X} \geq C \|(\mathbf{v}_h, \mathbf{w}_h, q_h)\|_{\mathcal{V}_h^X}$, with $(\mathbf{v}_h, \mathbf{w}_h, q_h) = (\beta \mathbf{u}_h^n + \pi_h \mathbf{v}_p, \beta \mathbf{z}_h^n, \beta p_h^n + \Delta t \nabla \cdot \mathbf{z}_h^n)$. Using the definition of the previously defined norms (15) and (16), we have

$$\begin{aligned} \|(\beta \mathbf{u}_h^n + \pi_h \mathbf{v}_p, \beta \mathbf{z}_h^n, \beta p_h^n + \Delta t \nabla \cdot \mathbf{z}_h^n)\|_{\mathcal{V}_h^X} &= \beta \|\mathbf{u}_h^n\|_{1,\Omega} + \|\pi_h \mathbf{v}_p\|_{1,\Omega} + \Delta t (1 + \beta) \|\nabla \cdot \mathbf{z}_h^n\|_{0,\Omega} \\ &\quad + \beta \Delta t^{1/2} \|\mathbf{z}_h^n\|_{0,\Omega} + \beta \|p_h^n\|_{0,\Omega} + \beta \|p_h^n\|_{J,\Omega} \\ &\leq C \|(\mathbf{u}_h^n, \mathbf{z}_h^n, p_h^n)\|_{\mathcal{W}_h^X}. \end{aligned}$$

This completes the proof. \square

3.2 Energy estimate of the fully-discrete model

In this section we construct two new combined bilinear forms, $B_{\delta t, h}^n$ (lemmas 3.2 and 3.3) and \mathcal{B}_h^n (lemmas 3.4 and 3.5). Lemmas 3.2 and 3.3 respectively develop a bound on $B_{\delta t, h}^n$, and an upper energy bound on the combined finite element formulation (27) with specially chosen test functions which combine to bound the displacements and pressure at time $T = N\Delta t$ in the H^1 -norm and J -norm respectively, and the pressures and fluxes in $\Omega \times (0, T]$ in the $l^2(L^2)$ norm. Lemmas 3.4 and 3.5 respectively develop a lower bound and an upper energy bound on (27) with specially chosen test functions which together bound the divergence of the flux in $\Omega \times (0, T]$ in the $l^2(L^2)$ norm. Since N is arbitrary, lemmas 3.3 and 3.5 can then be combined to bound the displacements and pressures in l^∞ in $(0, T]$ and the H^1 and J -norms respectively in Ω . Pressure, flux and the divergence of the flux are also all bounded in $\Omega \times (0, T]$ in the $l^2(L^2)$.

Adding (9a), (9b) and (9c), and assuming $p_D = 0$ on Γ_p and $\mathbf{t}_N = 0$ on Γ_t , we get the following

$$B_{\delta t, h}^n[(\mathbf{u}_h, \mathbf{z}_h, p_h), (\mathbf{v}_h, \mathbf{w}_h, q_h)] = (\mathbf{f}^n, \mathbf{v}_h) + (\mathbf{b}^n, \mathbf{w}_h) + (g^n, q_h) \quad \forall (\mathbf{v}_h, \mathbf{w}_h, q_h) \in \mathcal{W}_h^X, \quad (27)$$

where

$$\begin{aligned} B_{\delta t, h}^n[(\mathbf{u}_h, \mathbf{z}_h, p_h), (\mathbf{v}_h, \mathbf{w}_h, q_h)] &= a(\mathbf{u}_h^n, \mathbf{v}_h) + (\kappa^{-1} \mathbf{z}_h^n, \mathbf{w}_h) - (p_h^n, \nabla \cdot \mathbf{v}_h) - (p_h^n, \nabla \cdot \mathbf{w}_h) \\ &\quad + (\nabla \cdot \mathbf{u}_{\delta t, h}^n, q_h) + (\nabla \cdot \mathbf{z}_h^n, q_h) + J(p_{\delta t, h}^n, q_h). \end{aligned} \quad (28)$$

Lemma 3.2. *Let $\pi_h \mathbf{v}_p$ be the projection of some of $\mathbf{v}_p \in [H_0^1]^d$ onto \mathbf{W}_{h0}^E . Then for all $(\mathbf{u}_h^n, \mathbf{z}_h^n, p_h^n) \in (\mathbf{W}_h^E \times \mathbf{W}_h^D \times Q_h)$ the combined bilinear form (28) satisfies*

$$\begin{aligned} \sum_{n=0}^N \Delta t B_{\delta t, h}^n[(\mathbf{u}_h, \mathbf{z}_h, p_h), (\mathbf{u}_{\delta t, h}^n + \pi_h \mathbf{v}_p, \mathbf{z}_h^n, p_h^n)] &+ \|\mathbf{u}_h^0\|_{1,\Omega}^2 + \|\mathbf{u}_h\|_{l^2(H^1)}^2 + \|p_h\|_{l^2(J)}^2 \geq \\ &C \left(\|\mathbf{u}_h^N\|_{1,\Omega}^2 + \|p_h^N\|_{J,\Omega}^2 + \|\mathbf{z}_h\|_{l^2(L^2)}^2 + \|p_h\|_{l^2(L^2)}^2 \right). \end{aligned}$$

Proof. Choosing $\mathbf{v}_h = \mathbf{u}_{\delta t, h}^n + \pi_h \mathbf{v}_p$, $\mathbf{w}_h = \mathbf{z}_h^n$, $q_h = p_h^n$, with $\nabla \cdot \mathbf{v}_p = p_h^n$ in (28), multiplying by Δt , and summing over all time steps, we get

$$\begin{aligned} \sum_{n=1}^N \Delta t B_{\delta t, h}^n[(\mathbf{u}_h, \mathbf{z}_h, p_h), (\mathbf{u}_{\delta t, h}^n + \pi_h \mathbf{v}_p, \mathbf{z}_h^n, p_h^n)] &= \sum_{n=1}^N \Delta t a(\mathbf{u}_h^n, \mathbf{u}_{\delta t, h}^n) + \sum_{n=1}^N \Delta t a(\mathbf{u}_h^n, \pi_h \mathbf{v}_p) \\ &\quad - \sum_{n=1}^N \Delta t (p_h^n, \nabla \cdot \pi_h \mathbf{v}_p) + \sum_{n=1}^N \Delta t \kappa^{-1}(\mathbf{z}_h^n, \mathbf{z}_h^n) + \sum_{n=1}^N \Delta t J(p_{\delta t, h}^n, p_h^n). \end{aligned} \quad (29)$$

We now bound each of the above terms on the right hand side of (29) individually before combining the results.

$$\begin{aligned} \sum_{n=1}^N \Delta t a(\mathbf{u}_h^n, \mathbf{u}_{\delta t, h}^n) &= \sum_{n=1}^N \Delta t \left(\frac{1}{\Delta t} \|\mathbf{u}_h^n\|_{a, \Omega}^2 - \frac{1}{\Delta t} a(\mathbf{u}_h^n, \mathbf{u}_h^{n-1}) \right) \\ &\geq \frac{C_k}{2} \|\mathbf{u}_h^N\|_{1, \Omega}^2 - \frac{C_c}{2} \|\mathbf{u}_h^0\|_{1, \Omega}^2, \end{aligned} \quad (30)$$

where we have used (4) in the last step. Using (23) we have

$$\begin{aligned} \sum_{n=1}^N \Delta t a(\mathbf{u}_h^n, \pi_h \mathbf{v}_p) - \sum_{n=1}^N \Delta t (p_h^n, \nabla \cdot \pi_h \mathbf{v}_p) &\geq -\frac{C_c}{2\epsilon} \|\mathbf{u}_h\|_{l^2(H^1)}^2 + \left(1 - \left(\hat{c} + \frac{c_t}{2}\right) \frac{\epsilon}{2}\right) \|p_h\|_{l^2(L^2)}^2 \\ &\quad - \frac{1}{4\epsilon} \|p_h\|_{l^2(J)}^2. \end{aligned} \quad (31)$$

Using (5),

$$\sum_{n=1}^N \Delta t (\kappa^{-1}(\mathbf{z}_h^n, \mathbf{z}_h^n)) \geq \lambda_{max}^{-1} \|\mathbf{z}_h\|_{l^2(L^2)}^2. \quad (32)$$

The intermediate steps for the next bound have been omitted because they are very similar to (30). Thus

$$\sum_{n=1}^N \Delta t J(p_{\delta t, h}^n, p_h^n) \geq \frac{1}{2} \|p_h^N\|_{J, \Omega}^2. \quad (33)$$

We can now combine these intermediate results (30), (31), (32) and (33) to obtain from (29)

$$\begin{aligned} \sum_{n=0}^N \Delta t B_{\delta t, h}^n[(\mathbf{u}_h, \mathbf{z}_h, p_h), (\mathbf{u}_{\delta t, h}^n + \pi_h \mathbf{v}_p, \mathbf{z}_h^n, p_h^n)] &+ \frac{C_c}{2} \|\mathbf{u}_h^0\|_{1, \Omega}^2 + \frac{C_c}{2\epsilon} \|\mathbf{u}_h\|_{l^2(H^1)}^2 + \frac{1}{4\epsilon} \|p_h\|_{l^2(J)}^2 \\ &\geq \frac{C_k}{2} \|\mathbf{u}_h^N\|_{1, \Omega}^2 + \frac{1}{2} \|p_h^N\|_{J, \Omega}^2 + \lambda_{max}^{-1} \|\mathbf{z}_h\|_{l^2(L^2)}^2 + (1 - C\epsilon) \|p_h\|_{l^2(L^2)}^2. \end{aligned} \quad (34)$$

Finally choosing ϵ small completes the proof. \square

Lemma 3.3. *The combined finite element formulation (27) satisfies*

$$\|\mathbf{u}_h^N\|_{1, \Omega}^2 + \|p_h^N\|_{J, \Omega}^2 + \|\mathbf{z}_h\|_{l^2(L^2)}^2 + \|p_h\|_{l^2(L^2)}^2 \leq C.$$

Proof. Again choosing $\mathbf{v}_h = \mathbf{u}_{\delta t, h}^n + \pi_h \mathbf{v}_p$, $\mathbf{w}_h = \mathbf{z}_h^n$, $q_h = p_h^n$, with $\nabla \cdot \mathbf{v}_p = p_h^n$ in (27), multiplying by Δt , and summing yields

$$\begin{aligned} \sum_{n=1}^N \Delta t B_{\delta t, h}^n[(\mathbf{u}_h^n, \mathbf{z}_h^n, p_h^n), (\mathbf{u}_{\delta t, h}^n + \pi_h \mathbf{v}_p, \mathbf{z}_h^n, p_h^n)] &= \sum_{n=1}^N \Delta t(\mathbf{f}^n, \mathbf{u}_{\delta t, h}^n + \pi_h \mathbf{v}_p) \\ &+ \sum_{n=1}^N \Delta t(\mathbf{b}^n, \mathbf{z}_h^n) + \sum_{n=1}^N \Delta t(g^n, p_h^n). \end{aligned}$$

Let us note that,

$$\sum_{n=1}^N \Delta t(\mathbf{f}^n, \mathbf{u}_{\delta t, h}^n) = \sum_{n=1}^N (\mathbf{f}^n, \mathbf{u}_h^n - \mathbf{u}_h^{n-1}) = (\mathbf{f}^N, \mathbf{u}_h^N) - (\mathbf{f}^1, \mathbf{u}_h^0) - \sum_{n=1}^{N-1} (\mathbf{f}^{n+1} - \mathbf{f}^n, \mathbf{u}_h^n), \quad (35)$$

and further that

$$\begin{aligned} - \sum_{n=1}^{N-1} (\mathbf{f}^{n+1} - \mathbf{f}^n, \mathbf{u}_h^n) &\leq C \sum_{n=1}^{N-1} \|\mathbf{f}^{n+1} - \mathbf{f}^n\|_{0, \Omega} \|\mathbf{u}_h^n\|_{0, \Omega} \leq C \sum_{n=1}^{N-1} \left\{ \int_{t_n}^{t_{n+1}} \|\mathbf{f}_t\|_{0, \Omega} \right\}^{1/2} \|\mathbf{u}_h^n\|_{1, \Omega} \\ &\leq C \left(\frac{1}{2\epsilon} \|\mathbf{f}_t\|_{L^2(L^2)}^2 + \frac{\epsilon}{2} \|\mathbf{u}_h\|_{l^2(L^2)}^2 \right). \end{aligned}$$

Now using the above, lemma 3.2, the Cauchy-Schwarz and Young's inequalities, and noting (20), we arrive at

$$\begin{aligned} &(C - \frac{\epsilon}{2}) \|\mathbf{u}_h^N\|_{1, \Omega}^2 + C \|p_h^N\|_{J, \Omega}^2 + (C - \frac{\epsilon}{2}) \|\mathbf{z}_h\|_{l^2(L^2)}^2 + \left(C - \frac{\epsilon(1 + \hat{c})}{2} \right) \|p_h\|_{l^2(L^2)}^2 \\ &\leq \|\mathbf{u}_h\|_{l^2(H^1)}^2 + \|p_h\|_{l^2(J)}^2 + \frac{1}{2\epsilon} \|\mathbf{f}^N\|_{0, \Omega}^2 + \frac{C}{2\epsilon} \|\mathbf{f}_t\|_{L^2(L^2)}^2 + (1 + \frac{C\epsilon}{2}) \|\mathbf{u}_h\|_{l^2(L^2)}^2 + (1 + \frac{\epsilon}{2}) \|\mathbf{u}_h^0\|_{0, \Omega}^2 \\ &\quad + \frac{1}{2\epsilon} \|\mathbf{f}^0\|_{l^2(L^2)}^2 + \frac{1}{2\epsilon} \|\mathbf{f}\|_{l^2(L^2)}^2 + \frac{1}{2\epsilon} \|\mathbf{b}\|_{l^2(L^2)}^2 + \frac{1}{2\epsilon} \|g\|_{l^2(L^2)}^2. \end{aligned}$$

Finally, choosing ϵ sufficiently small, applying a discrete version of Gronwall's lemma, using (7a), (7b), (7c) and (8), we arrive at the desired result. \square

To get a bound for the fluid flux in its natural *Hdiv* norm we now define another combined bilinear form \mathcal{B}_h^n . We first show how we derive \mathcal{B}_h^n from the fully-discrete weak form (9), for which we know that a solution $(\mathbf{u}_h, \mathbf{z}_h, p_h)$ exists for test functions $(\mathbf{v}_h, \mathbf{w}_h, q_h) \in \mathcal{V}_h^X$. Adding (9a) and (9b), assuming $p_D = 0$ on Γ_p and $\mathbf{t}_N = 0$ on Γ_t , and summing we have

$$\begin{aligned} \sum_{n=1}^N a(\mathbf{u}_h^n, \mathbf{v}_h) + \sum_{n=1}^N (\kappa^{-1} \mathbf{z}_h^n, \mathbf{w}_h) - \sum_{n=1}^N (p_h^n, \nabla \cdot \mathbf{v}_h) - \sum_{n=1}^N (p_h^n, \nabla \cdot \mathbf{w}_h) \\ = \sum_{n=1}^N (\mathbf{f}^n, \mathbf{v}_h) + \sum_{n=1}^N (\mathbf{b}^n, \mathbf{w}_h) \quad \forall (\mathbf{v}_h, \mathbf{w}_h, q_h) \in \mathcal{V}_h^X. \quad (36) \end{aligned}$$

Adding (9a) and (9b), assuming $p_D = 0$ on Γ_p and $\mathbf{t}_N = 0$ on Γ_t , summing from 0 to $N - 1$, and introducing an initial condition for the fluid flux $\mathbf{z}_h^0 = \mathbf{z}^0$, we have

$$\begin{aligned} \sum_{n=1}^N a(\mathbf{u}_h^{n-1}, \mathbf{v}_h) + \sum_{n=1}^N (\kappa^{-1} \mathbf{z}_h^{n-1}, \mathbf{w}_h) - \sum_{n=1}^N (p_h^{n-1}, \nabla \cdot \mathbf{v}_h) - \sum_{n=1}^N (p_h^{n-1}, \nabla \cdot \mathbf{w}_h) \\ = \sum_{n=1}^N (\mathbf{f}^{n-1}, \mathbf{v}_h) + \sum_{n=1}^N (\mathbf{b}^{n-1}, \mathbf{w}_h) \quad \forall (\mathbf{v}_h, \mathbf{w}_h, q_h) \in \mathcal{V}_h^X. \end{aligned} \quad (37)$$

Taking (9c), multiplying by Δt , and summing we have

$$\sum_{n=1}^N \Delta t (\nabla \cdot \mathbf{u}_{\delta t, h}^n, q_h) + \sum_{n=1}^N \Delta t (\nabla \cdot \mathbf{z}_h^n, q_h) + \sum_{n=1}^N \Delta t J(p_{\delta t, h}^n, q_h) = \sum_{n=1}^N \Delta t (g^n, q_h) \quad \forall (\mathbf{v}_h, \mathbf{w}_h, q_h) \in \mathcal{V}_h^X. \quad (38)$$

Now adding (36) and (38), and subtracting (37) we get

$$\begin{aligned} \sum_{n=1}^N \Delta t \mathcal{B}_h^n[(\mathbf{u}_h, \mathbf{z}_h, p_h), (\mathbf{v}_h, \mathbf{w}_h, q_h)] &= \sum_{n=1}^N \Delta t (\mathbf{f}_{\delta t}^n, \mathbf{v}_h) + \sum_{n=1}^N \Delta t (\mathbf{b}_{\delta t}^n, \mathbf{w}_h) \\ &+ \sum_{n=1}^N \Delta t (g^n, q_h) \quad \forall (\mathbf{v}_h, \mathbf{w}_h, q_h) \in \mathcal{V}_h^X, \end{aligned} \quad (39)$$

where

$$\begin{aligned} \mathcal{B}_h^n[(\mathbf{u}_h, \mathbf{z}_h, p_h), (\mathbf{v}_h, \mathbf{w}_h, q_h)] &= a(\mathbf{u}_{\delta t, h}^n, \mathbf{v}_h) + (\kappa^{-1} \mathbf{z}_{\delta t, h}^n, \mathbf{w}_h) - (p_{\delta t, h}^n, \nabla \cdot \mathbf{v}_h) - (p_{\delta t, h}^n, \nabla \cdot \mathbf{w}_h) \\ &+ (\nabla \cdot \mathbf{u}_{\delta t, h}^n, q_h) + (\nabla \cdot \mathbf{z}_h^n, q_h) + J(p_{\delta t, h}^n, q_h). \end{aligned} \quad (40)$$

Lemma 3.4. *Let $\beta > 0$ and $\pi_h \mathbf{v}_p$ be the projection of some of $\mathbf{v}_p \in [H_0^1]^d$ onto \mathbf{W}_{h0}^E . Then for all $(\mathbf{u}_h^n, \mathbf{z}_h^n, p_h^n) \in (\mathbf{W}_h^E \times \mathbf{W}_h^D \times Q_h)$ the combined bilinear form (40) satisfies*

$$\begin{aligned} \sum_{n=1}^N \Delta t \mathcal{B}_h^n[(\mathbf{u}_h, \mathbf{z}_h, p_h), (\beta \mathbf{u}_{\delta t, h}^n + \pi_h \mathbf{v}_p, \beta \mathbf{z}_h^n, \beta p_{\delta t, h}^n + \nabla \cdot \mathbf{z}_h^n)] &\geq \\ C \left(\|\mathbf{u}_{\delta t, h}\|_{l^2(H^1)}^2 + \|\mathbf{z}_h^N\|_{0, \Omega}^2 + \|p_{\delta t, h}\|_{l^2(L^2)}^2 + \|p_{\delta t, h}\|_{l^2(J)}^2 + \|\nabla \cdot \mathbf{z}_h\|_{l^2(L^2)}^2 \right). \end{aligned}$$

Proof. Choosing $\mathbf{v}_h = \beta \mathbf{u}_{\delta t, h}^n + \pi_h \mathbf{v}_p$, $\mathbf{w}_h = \beta \mathbf{z}_h^n$, $q_h = \beta p_{\delta t, h}^n + \nabla \cdot \mathbf{z}_h^n$, with $\nabla \cdot \mathbf{v}_p = p_{\delta t, h}$ in (40) we get

$$\begin{aligned} \sum_{n=1}^N \Delta t \mathcal{B}_h^n[(\mathbf{u}_h, \mathbf{z}_h, p_h), (\beta \mathbf{u}_{\delta t, h}^n + \pi_h \mathbf{v}_p, \beta \mathbf{z}_h^n, \beta p_{\delta t, h}^n + \nabla \cdot \mathbf{z}_h^n)] \\ = \sum_{n=1}^N \Delta t a(\mathbf{u}_{\delta t, h}^n, \beta \mathbf{u}_{\delta t, h}^n) + \sum_{n=1}^N \Delta t \kappa^{-1} (\mathbf{z}_{\delta t, h}^n, \beta \mathbf{z}_h^n) + \sum_{n=1}^N \Delta t (\nabla \cdot \mathbf{z}_h^n, \nabla \cdot \mathbf{z}_h^n) + \sum_{n=1}^N \Delta t (\mathbf{u}_{\delta t, h}^n, \nabla \cdot \mathbf{z}_h^n) \\ + \sum_{n=1}^N \Delta t J(p_{\delta t, h}^n, \nabla \cdot \mathbf{z}_h^n) + \sum_{n=1}^N \Delta t J(p_{\delta t, h}^n, \beta p_{\delta t, h}^n) + \sum_{n=1}^N \Delta t a(\mathbf{u}_{\delta t, h}^n, \pi_h \mathbf{v}_p) - \sum_{n=1}^N \Delta t (p_{\delta t, h}^n, \nabla \cdot \pi_h \mathbf{v}_p). \end{aligned} \quad (41)$$

We now give some individual intermediate bounds for the above terms on the right hand side of (41) before combining the results.

$$\sum_{n=1}^N \Delta t a(\mathbf{u}_{\delta t, h}^n, \beta \mathbf{u}_{\delta t, h}^n) \geq \beta C_k \|\mathbf{u}_{\delta t, h}^n\|_{l^2(H^1)}^2, \quad (42)$$

where we have used (4). Next using (5) we have

$$\sum_{n=1}^N \Delta t \kappa^{-1}(\mathbf{z}_{\delta t, h}^n, \beta \mathbf{z}_h^n) \geq \frac{\beta \lambda_{max}^{-1}}{2} \|\mathbf{z}_h^N\|_{0, \Omega}^2 - \frac{\beta \lambda_{min}^{-1}}{2} \|\mathbf{z}_h^0\|_{0, \Omega}^2. \quad (43)$$

Using the Cauchy-Schwarz, Young's and the Poincaré inequalities we have

$$\sum_{n=1}^N \Delta t (\mathbf{u}_{\delta t, h}^n, \nabla \cdot \mathbf{z}_h^n) \leq \frac{C_p}{2\epsilon} \|\mathbf{u}_{\delta t, h}\|_{l^2(H^1)}^2 + \frac{\epsilon}{2} \|\nabla \cdot \mathbf{z}_h\|_{l^2(L^2)}^2. \quad (44)$$

Again using the Cauchy-Schwarz and Young's inequalities and (24) we have

$$\Delta t J(p_{\delta t, h}^n, \nabla \cdot \mathbf{z}_h^n) \leq \frac{1}{2\epsilon} \|p_{\delta t, h}\|_{l^2(J)}^2 + \epsilon c_z \|\nabla \cdot \mathbf{z}_h\|_{l^2(L^2)}^2. \quad (45)$$

Using an approach very similar to step 2 in the proof of Theorem 3.1 we have

$$\begin{aligned} \sum_{n=1}^N \Delta t a(\mathbf{u}_{\delta t, h}^n, \pi_h \mathbf{v}_p) - \sum_{n=1}^N \Delta t (p_{\delta t, h}^n, \nabla \cdot \pi_h \mathbf{v}_p) &\geq -\frac{C_c}{2\epsilon} \|\mathbf{u}_{th}\|_{l^2(H^1)}^2 + (1 - C\epsilon) \|p_{\delta t, h}\|_{l^2(L^2)}^2 \\ &\quad - \frac{1}{4\epsilon} \|p_{\delta t, h}\|_{l^2(J)}^2. \end{aligned} \quad (46)$$

We can now combine these intermediate results to obtain the following result

$$\begin{aligned} \sum_{n=1}^N \Delta t \mathcal{B}_h^n[(\mathbf{u}_h, \mathbf{z}_h, p_h), (\beta \mathbf{u}_{\delta t, h}^n + \pi_h \mathbf{v}_p, \beta \mathbf{z}_h^n, \beta p_{\delta t, h}^n + \nabla \cdot \mathbf{z}_h^n)] &\geq \left(\beta C_k - \frac{C_p + C_c}{2\epsilon} \right) \|\mathbf{u}_{\delta t, h}\|_{l^2(H^1)}^2 \\ &\quad + \frac{\beta \lambda_{max}^{-1}}{2} \|\mathbf{z}_h^N\|_{0, \Omega}^2 + \left(\beta - \frac{3}{4\epsilon} \right) \|p_{\delta t, h}\|_{l^2(J)}^2 + (1 - \epsilon(1 + c_z)) \|\nabla \cdot \mathbf{z}_h\|_{l^2(L^2)}^2 \\ &\quad - \frac{\beta \lambda_{min}^{-1}}{2} \|\mathbf{z}_h^0\|_{0, \Omega}^2 + (1 - C\epsilon) \|p_{\delta t, h}\|_{l^2(L^2)}^2. \end{aligned} \quad (47)$$

Finally choosing ϵ small, $\beta \geq \max \left[\frac{C_p}{2C_k\epsilon}, \frac{3}{4\epsilon} \right]$, and using (8), completes the proof. \square

Lemma 3.5. *The combined finite element formulation (39) satisfies*

$$\|\nabla \cdot \mathbf{z}_h\|_{l^2(L^2)}^2 \leq C.$$

Proof. Choosing $\mathbf{v}_h = \beta \mathbf{u}_{\delta t, h}^n + \pi_h \mathbf{v}_p$, $\mathbf{w}_h = \beta \mathbf{z}_h^n$, $q_h = \beta p_{\delta t, h}^n + \nabla \cdot \mathbf{z}_h^n$ in (39), multiplying by Δt , and summing yields

$$\begin{aligned} \sum_{n=1}^N \Delta t \mathcal{B}_h^n[(\mathbf{u}_h^n, \mathbf{z}_h^n, p_h^n), (\beta \mathbf{u}_{\delta t, h}^n + \pi_h \mathbf{v}_p, \mathbf{z}_h^n, \beta p_{\delta t, h}^n + \nabla \cdot \mathbf{z}_h^n)] &= \sum_{n=1}^N \Delta t (\mathbf{f}_{\delta t}^n, \mathbf{u}_{\delta t, h}^n) + \sum_{n=1}^N \Delta t (\mathbf{b}_{\delta t}^n, \beta \mathbf{z}_h^n) \\ &\quad + \sum_{n=1}^N \Delta t (g^n, \beta p_{\delta t, h}^n). \end{aligned}$$

Here β is a constant that is chosen to be the same as in lemma 3.4. Using lemma 3.4, the Cauchy-Schwarz and Young's inequalities, noting (11), along with ideas already presented in the proof of lemma 3.3 we arrive at

$$\begin{aligned} \|\mathbf{u}_{\delta t, h}\|_{l^2(H^1)}^2 + (1 - C\epsilon)\|p_{\delta t, h}\|_{l^2(L^2)}^2 + \|p_{\delta t, h}\|_{l^2(J)}^2 + \|\mathbf{z}_h^N\|_{0, \Omega}^2 + \|\nabla \cdot \mathbf{z}_h\|_{l^2(L^2)}^2 \\ \leq C \left(\|\mathbf{f}_t\|_{L^2(L^2)}^2 + \|\mathbf{u}_{\delta t, h}\|_{l^2(L^2)}^2 + \|\mathbf{b}_t\|_{L^2(L^2)}^2 + \|\mathbf{z}_h\|_{l^2(L^2)}^2 + \frac{1}{\epsilon}\|g\|_{L^2(L^2)}^2 \right). \end{aligned}$$

Finally applying a discrete version of Gronwall's lemma, using (7a), (7b), (7c), and choosing ϵ small, we arrive at the desired result. \square

Theorem 3.6. *The fully-discrete problem (9) satisfies the energy estimate*

$$\|\mathbf{u}_h\|_{l^\infty(H^1)}^2 + \|p_h\|_{l^\infty(J)}^2 + \|\mathbf{z}_h\|_{l^2(L^2)}^2 + \|p_h\|_{l^2(L^2)}^2 + \|\nabla \cdot \mathbf{z}_h\|_{l^2(L^2)}^2 \leq C.$$

Proof. The proof follows from combining lemma 3.3 and lemma 3.5, and noting that these lemmas hold for all time steps $n = 0, 1, \dots, N$. This then gives the desired discrete in time l^∞ bounds. \square

Remark 1. *Having proven Theorem 3.6, it is now a standard calculation to show that the discrete Galerkin approximation converges weakly, as $\Delta t, h \rightarrow 0$, to the continuous problem with respect to continuous versions of the norms of the energy estimate in Theorem 3.6. This in turn shows that the continuous variational problem is well-posed. Due to the linearity of the variational form and noting that $\|\mathbf{v}\|_{J, \Omega} \rightarrow 0$ as $h \rightarrow 0$, these calculations are straight forward and closely follow the existence and uniqueness proofs presented in Ženíšek [1984] and Barucq et al. [2005] for the linear two-field Biot problem and a nonlinear Biot problem, respectively.*

4 A-priori error analysis

We now derive an a-priori error estimate for the fully-discrete model. We start by introducing some notation, and then give a Galerkin orthogonality result which will form the corner stone of the error analysis. Lemma 4.1 provides a Galerkin orthogonality result obtained by comparing continuous and discrete weak forms. Lemma 4.2 is a standard approximation result for projections. Lemma 4.3 bounds the auxiliary errors for displacement, flux and pressure in the appropriate norms. Lemma 4.4 bounds the auxiliary error for the divergence of the flux. Since Lemmas 4.3 and 4.4 bound the auxiliary errors at the same order as the approximation errors, combining projection and auxiliary errors in Theorem 4.5 provides an optimal error estimate. To simplify the notation we introduce the following interpolation errors:

$$\eta_{\mathbf{u}}^n := \mathbf{u}(t_n) - \pi_h \mathbf{u}(t_n), \quad \eta_{\mathbf{u}_t}^n := \mathbf{u}_t(t_n) - \pi_h \mathbf{u}_t(t_n), \quad \eta_{\mathbf{z}}^n := \mathbf{z}(t_n) - \pi_h \mathbf{z}(t_n), \quad \eta_p^n := p(t_n) - \pi_h p(t_n), \quad (48)$$

auxiliary errors:

$$\theta_{\mathbf{u}}^n := \pi_h \mathbf{u}(t_n) - \mathbf{u}_h^n, \quad \theta_{\mathbf{z}}^n := \pi_h \mathbf{z}(t_n) - \mathbf{z}_h^n, \quad \theta_p^n := \pi_h p(t_n) - p_h^n, \quad (49)$$

and time-discretization errors:

$$\rho_{\mathbf{u}}^n := \frac{\mathbf{u}(t_n) - \mathbf{u}(t_{n-1})}{\Delta t} - \frac{\partial \mathbf{u}(t_n)}{\partial t}, \quad \rho_p^n := \frac{p(t_n) - p(t_{n-1})}{\Delta t} - \frac{\partial p(t_n)}{\partial t}. \quad (50)$$

4.1 Galerkin orthogonality

We now give a Galerkin orthogonality type argument for analysing the difference between the fully-discrete approximation and the true solution. For this we introduce the continuous counterpart of the fully-discrete combined weak form (27) given by

$$B^n[(\mathbf{u}, \mathbf{z}, p), (\mathbf{v}, \mathbf{w}, q)] = (\mathbf{f}(t_n), \mathbf{v}) + (\mathbf{t}_N(t_n), \mathbf{v})_{\Gamma_t} + (\mathbf{b}(t_n), \mathbf{w}) - (p_D, \mathbf{w} \cdot \mathbf{n})_{\Gamma_p} + (g(t_n), q) \quad \forall (\mathbf{v}, \mathbf{w}, q) \in \mathcal{V}_h^X, \quad (51)$$

where

$$B^n[(\mathbf{u}, \mathbf{z}, p), (\mathbf{v}, \mathbf{w}, q)] = a(\mathbf{u}(t_n), \mathbf{v}) + \kappa^{-1}(\mathbf{z}(t_n), \mathbf{w}) - (p(t_n), \nabla \cdot \mathbf{v}) - (p(t_n), \nabla \cdot \mathbf{w}) + (\nabla \cdot \mathbf{u}_t(t_n), q) + (\nabla \cdot \mathbf{z}(t_n), q). \quad (52)$$

Lemma 4.1. *If $(\mathbf{u}(t_n), \mathbf{z}(t_n), p(t_n))$ is a solution to (51) with $(\mathbf{u}(t_n), \mathbf{z}(t_n), p(t_n)) \in \mathbf{W}^E \times \mathbf{W}^D \times H^1(\Omega) \cap \mathcal{L}(\Omega)$ then*

$$B_{\delta t, h}^n[(\mathbf{u} - \mathbf{u}_h, \mathbf{z} - \mathbf{z}_h, p - p_h), (\mathbf{v}_h, \mathbf{w}_h, q_h)] = (\nabla \cdot \rho_{\mathbf{u}}^n, q_h) + J(\rho_p^n, q_h) \quad \forall (\mathbf{v}_h, \mathbf{w}_h, q_h) \in \mathcal{V}_h^X.$$

Proof. Subtracting the discrete weak form (27) from the continuous weak form (51), and assuming $p_D = 0$ on Γ_p and $\mathbf{t}_N = 0$ on Γ_t , we have

$$B^n[(\mathbf{u}, \mathbf{z}, p), (\mathbf{v}_h, \mathbf{w}_h, q_h)] - B_{\delta t, h}^n[(\mathbf{u}_h, \mathbf{z}_h, p_h), (\mathbf{v}_h, \mathbf{w}_h, q_h)] = 0,$$

which gives us

$$a(\mathbf{u}(t_n) - \mathbf{u}_h^n, \mathbf{v}_h) + (\kappa^{-1}(\mathbf{z}(t_n) - \mathbf{z}_h^n), \mathbf{w}_h) - (p(t_n) - p_h^n, \nabla \cdot \mathbf{v}_h) - (p(t_n) - p_h^n, \nabla \cdot \mathbf{w}_h) + (\nabla \cdot (\mathbf{z}(t_n) - \mathbf{z}_h^n), q_h^n) + (\nabla \cdot (\mathbf{u}_t(t_n) - \mathbf{u}_{\delta t, h}^n), q_h) - J(p_{\delta t, h}^n, q_h) = 0.$$

Now add $J(p_t(t_n), q) = 0$ to the left hand side. Here we have made the additional assumption that $p(t_n) \in H^1(\Omega)$, so that $[p_t(t_n)] = 0$ (see lemma 1.23 in Di Pietro and Ern [2011]). Also add $(\nabla \cdot (\mathbf{u}_{\delta t}(t_n) - \mathbf{u}_t(t_n)), q) + J(p_{\delta t}(t_n) - p_t(t_n), q)$ to the left and the right hand side to yield

$$a(\mathbf{u}(t_n) - \mathbf{u}_h^n, \mathbf{v}) + (\kappa^{-1}(\mathbf{z}(t_n) - \mathbf{z}_h^n), \mathbf{w}_h) - (p(t_n) - p_h^n, \nabla \cdot \mathbf{v}_h) - (p(t_n) - p_h^n, \nabla \cdot \mathbf{w}_h) + (\nabla \cdot (\mathbf{z}(t_n) - \mathbf{z}_h^n), q) + (\nabla \cdot (\mathbf{u}_{\delta t}(t_n) - \mathbf{u}_{\delta t, h}^n), q) + J(p_{\delta t}(t_n) - p_{\delta t, h}^n, q_h) = (\nabla \cdot (\mathbf{u}_{\delta t}(t_n) - \mathbf{u}_t(t_n)), q_h) + J(p_{\delta t}(t_n) - p_t(t_n), q_h). \quad (53)$$

The result now follows. \square

4.2 Approximation results

We will now give some approximation results that will be useful later.

Lemma 4.2. *The projection operator π_h has the following approximation property for functions $(\mathbf{u}(t_n), \mathbf{z}(t_n), p(t_n)) \in [H^2(\Omega)]^d \times [H^1(\Omega)]^d \times H^1(\Omega)$:*

$$\|\eta_{\mathbf{u}}^n\|_{1, \Omega} \leq Ch\|\mathbf{u}^n\|_{2, \Omega}, \quad \|\eta_{\mathbf{z}}^n\|_{0, \Omega} \leq Ch\|\mathbf{z}^n\|_{1, \Omega}, \quad \|\eta_p^n\|_{0, \Omega} \leq Ch\|p^n\|_{1, \Omega}. \quad (54)$$

We also have the following approximation for the time-discretization error:

$$\sum_{n=1}^N \Delta t \|\rho_{\mathbf{u}}^n\|_{0, \Omega}^2 \leq \Delta t^2 \int_0^{t_N} \|\mathbf{u}_{tt}\|_{0, \Omega}^2 ds. \quad (55)$$

Proof. Straight from standard approximation theory in Brenner and Scott [2008] and Thomée [2006]. \square

4.3 Auxiliary error estimates on displacement, fluid flux and pressure

Lemma 4.3. Assume that the true solution $(\mathbf{u}, \mathbf{z}, p)$ is in $H^2 \left([H^2(\Omega)]^d \right) \times l^2 \left([H^1(\Omega)]^d \right) \times H^2 \left(H^1(\Omega) \cap \mathcal{L}(\Omega) \right)$, then the finite element solution (9) satisfies the error estimate

$$\begin{aligned} & \|\theta_{\mathbf{u}}\|_{l^\infty(H^1)} + \|\theta_{\mathbf{z}}\|_{l^2(L^2)} + \|\theta_p\|_{l^\infty(L^2)} + \|\theta_p\|_{l^\infty(J)} \\ & \leq Ch \left(\|p_t\|_{l^2(H^1)} + \|\mathbf{u}\|_{l^\infty(H^2)}^2 + \|\mathbf{u}_t\|_{l^2(H^2)} + \|\mathbf{z}\|_{l^2(H^1)} \right) + Ch\Delta t \left(\|\mathbf{u}_{tt}\|_{L^2(H^2)} + \|p_{tt}\|_{L^2(H^1)} \right) \\ & \quad + C\Delta t \left(\|p_{tt}\|_{L^2(L^2)}^2 + \|\nabla \cdot \mathbf{u}_{tt}\|_{L^2(L^2)}^2 \right). \end{aligned}$$

Proof. From the Galerkin orthogonality result, lemma 4.1, we have

$$\begin{aligned} & a(\mathbf{u}^n - \mathbf{u}_h^n, \mathbf{v}_h) + (\kappa^{-1}(\mathbf{z}^n - \mathbf{z}_h^n), \mathbf{w}_h) - (p^n - p_h^n, \nabla \cdot \mathbf{v}_h) - (p^n - p_h^n, \nabla \cdot \mathbf{w}_h) \\ & \quad + (q_h, \nabla \cdot (\mathbf{z}^n - \mathbf{z}_h^n)) + (q_h, \nabla \cdot (\mathbf{u}_{\delta t}(t_n) - \mathbf{u}_{\delta t,h}^n)) + J(p_{\delta t}(t_n) - p_{\delta t,h}^n, q_h) \\ & \quad = (\nabla \cdot \rho_{\mathbf{u}}^n, q_h) + J(\rho_p^n, q_h). \end{aligned}$$

Using the definitions of the interpolation error (48) and the auxiliary error (49), and choosing $\mathbf{v}_h = \theta_{\delta t, \mathbf{u}}^n + \pi_h \mathbf{v}_p$, $\mathbf{w}_h = \theta_{\mathbf{z}}^n$, $q_h = \theta_p^n$, with $-\nabla \cdot \mathbf{v}_p = \theta_p^n$, we get

$$\begin{aligned} & a(\theta_{\mathbf{u}}^n + \eta_{\mathbf{u}}^n, \theta_{\delta t, \mathbf{u}}^n + \pi_h \mathbf{v}_p) + (\kappa^{-1}(\theta_{\mathbf{z}}^n + \eta_{\mathbf{z}}^n), \theta_{\mathbf{z}}^n) - (\theta_p^n + \eta_p^n, \nabla \cdot (\theta_{\delta t, \mathbf{u}}^n + \pi_h \mathbf{v}_p)) - (\theta_p^n + \eta_p^n, \nabla \cdot \theta_{\mathbf{z}}^n) \\ & \quad + (\theta_p^n, \nabla \cdot (\theta_{\mathbf{z}}^n + \eta_{\mathbf{z}}^n)) + (\theta_p^n, \nabla \cdot (\theta_{\delta t, \mathbf{u}}^n + \eta_{\delta t, \mathbf{u}}^n)) + J(\theta_{\delta t, p}^n + \eta_{\delta t, p}^n, \theta_p^n) \\ & \quad = (\nabla \cdot \rho_{\mathbf{u}}^n, \theta_p^n) + J(\rho_p^n, \theta_p^n). \end{aligned}$$

Rearranging, noting that $(\eta_p^n, \nabla \cdot \theta_{\delta t, \mathbf{u}}^n + \pi_h \mathbf{v}_p) = (\eta_p^n, \nabla \cdot \theta_{\mathbf{z}}^n) = 0$ due to the properties of the projection operator, both sides by Δt and summing we have

$$\begin{aligned} & \sum_{n=1}^N \Delta t a(\theta_{\mathbf{u}}^n, \theta_{\delta t, \mathbf{u}}^n) + \sum_{n=1}^N \Delta t (\kappa^{-1}(\theta_{\mathbf{z}}^n, \theta_{\mathbf{z}}^n)) + \sum_{n=1}^N \Delta t a(\theta_{\mathbf{u}}^n, \pi_h \mathbf{v}_p) - \sum_{n=1}^N \Delta t (\theta_p^n, \nabla \cdot \pi_h \mathbf{v}_p) \\ & \quad + \sum_{n=1}^N \Delta t J(\theta_{\delta t, p}^n, \theta_p^n) = \Phi_1 + \Phi_2 + \Phi_3 + \Phi_4 + \Phi_5 + \Phi_6 + \Phi_7. \quad (56) \end{aligned}$$

where

$$\begin{aligned} \Phi_1 &= - \sum_{n=1}^N \Delta t a(\eta_{\mathbf{u}}^n, \theta_{\delta t, \mathbf{u}}^n), & \Phi_2 &= - \sum_{n=1}^N \Delta t (\kappa^{-1}(\eta_{\mathbf{z}}^n, \theta_{\mathbf{z}}^n)), & \Phi_3 &= - \sum_{n=1}^N \Delta t a(\eta_{\mathbf{u}}^n, \pi_h \mathbf{v}_p), \\ \Phi_4 &= - \sum_{n=1}^N \Delta t J(\eta_{\delta t, p}^n, \theta_p^n), & \Phi_5 &= \sum_{n=1}^N \Delta t (\nabla \cdot \rho_{\mathbf{u}}^n, \theta_p^n), & \Phi_6 &= \sum_{n=1}^N \Delta t J(\rho_p^n, \theta_p^n), \\ \Phi_7 &= - \sum_{n=1}^N \Delta t (\theta_p^n, \eta_{\delta t, \mathbf{u}}^n + \eta_{\mathbf{z}}^n). \end{aligned}$$

Using (34) we can immediately bound the left hand side terms of (56) below, namely

$$\begin{aligned}
& \frac{C_k}{2} \|\theta_{\mathbf{u}}^N\|_{1,\Omega}^2 + \frac{1}{2} \|\theta_p^N\|_{J,\Omega}^2 + \lambda_{max}^{-1} \|\theta_{\mathbf{z}}\|_{l^2(L^2)}^2 + (1 - C\epsilon) \|\theta_p\|_{l^2(L^2)}^2 - \frac{C_c}{2\epsilon} \|\theta_{\mathbf{u}}\|_{l^2(H^1)}^2 - \frac{1}{4\epsilon} \|\theta_p\|_{l^2(J)}^2 \\
& \leq \sum_{n=1}^N \Delta t a(\theta_{\mathbf{u}}^n, \theta_{\delta t, \mathbf{u}}^n) + \sum_{n=1}^N \Delta t (\kappa^{-1}(\theta_{\mathbf{z}}^n, \theta_{\mathbf{z}}^n)) + \sum_{n=1}^N \Delta t a(\theta_{\mathbf{u}}^n, \pi_h \mathbf{v}_p) \\
& \quad - \sum_{n=1}^N \Delta t (\theta_p^n, \nabla \cdot \pi_h \mathbf{v}_p) + \sum_{n=1}^N \Delta t J(\theta_{\delta t, p}^n, \theta_p^n). \quad (57)
\end{aligned}$$

Here we have also used that $\theta_{\mathbf{u}}^0 = 0$ due to (10a).

We now consider the terms on the right hand side of (56). We will bound these primarily using the Cauchy-Schwarz and Young's inequalities. To bound the first quantity, we use (35), lemma 4.2, the Cauchy-Schwarz and Young's inequalities, $\theta_{\mathbf{u}}^0 = 0$, and (4),

$$\begin{aligned}
\Phi_1 &= - \sum_{n=1}^N a(\eta_{\mathbf{u}}^n, \theta_{\mathbf{u}}^n - \theta_{\mathbf{u}}^{n-1}) \\
&= -a(\eta_{\mathbf{u}}^N, \theta_{\mathbf{u}}^N) + \sum_{n=1}^N a(\eta_{\mathbf{u}}^n - \eta_{\mathbf{u}}^{n-1}, \theta_{\mathbf{u}}^{n-1}) \\
&= -a(\eta_{\mathbf{u}}^N, \theta_{\mathbf{u}}^N) + \Delta t \sum_{n=1}^N a(\eta_{\mathbf{u}_t}^n, \theta_{\mathbf{u}}^{n-1}) + \sum_{n=1}^N a\left(\int_{t_{n-1}}^{t_n} (s - t_{n-1}) \eta_{\mathbf{u}_{tt}} ds, \theta_{\mathbf{u}}^{n-1}\right) \\
&\leq \frac{\epsilon C_c}{2} \|\theta_{\mathbf{u}}^N\|_{1,\Omega}^2 + \frac{C_c}{2\epsilon} \|\eta_{\mathbf{u}}^N\|_{1,\Omega}^2 + \epsilon C_c \|\theta_{\mathbf{u}}\|_{l^2(H^1)}^2 + \frac{C_c}{2\epsilon} \|\eta_{\mathbf{u}_t}\|_{l^2(H^1)}^2 + \frac{C_c}{2\epsilon} \Delta t^2 \int_0^{t_N} \|\eta_{\mathbf{u}_{tt}}\|_{1,\Omega}^2 ds. \quad (58)
\end{aligned}$$

Next, using (5), and Young's inequality,

$$\Phi_2 \leq \frac{\epsilon}{2} \|\theta_{\mathbf{z}}\|_{l^2(L^2)}^2 + \frac{\lambda_{min}^{-2}}{2\epsilon} \|\eta_{\mathbf{z}}^n\|_{l^2(L^2)}^2. \quad (59)$$

Again using (4), Young's inequality, and (20),

$$\Phi_3 \leq \frac{\epsilon}{2} \|\pi_h \mathbf{v}_p\|_{l^2(H^1)}^2 + \frac{C_c^2}{2\epsilon} \|\eta_{\mathbf{u}}\|_{l^2(H^1)}^2 \leq \frac{\epsilon \hat{c}^2}{2} \|\theta_p\|_{l^2(L^2)}^2 + \frac{C_c^2}{2\epsilon} \|\eta_{\mathbf{u}}^n\|_{l^2(H^1)}^2. \quad (60)$$

The bound on Φ_4 is obtained using a similar argument to the bound on Φ_1 ,

$$\Phi_4 \leq \epsilon \|\theta_p\|_{l^2(J)}^2 + \frac{1}{2\epsilon} \|\eta_{p_t}\|_{l^2(J)}^2 + \frac{\Delta t^2}{2\epsilon} \int_0^{t_N} \|\eta_{p_{tt}}\|_{J,\Omega}^2 ds. \quad (61)$$

Using the Cauchy-Schwarz and Young's inequalities and lemma 4.2,

$$\Phi_5 \leq \frac{\epsilon}{2} \|\theta_p\|_{l^2(L^2)}^2 + \frac{1}{2\epsilon} \sum_{n=1}^N \Delta t \|\nabla \cdot \rho_{\mathbf{u}}^n\|_{0,\Omega}^2 \leq \frac{\epsilon}{2} \|\theta_p\|_{l^2(L^2)}^2 + \frac{\Delta t^2}{2\epsilon} \int_0^{t_N} \|\nabla \cdot \mathbf{u}_{tt}\|_{0,\Omega}^2 ds. \quad (62)$$

Similarly we have

$$\Phi_6 \leq \frac{\epsilon}{2} \|\theta_p\|_{l^2(J)}^2 + \frac{\Delta t^2}{2\epsilon} \int_0^{t_N} \|p_{tt}\|_{J,\Omega}^2 ds. \quad (63)$$

Using the Cauchy-Schwarz and Young's inequalities, and a similar argument to the bound on Φ_1 ,

$$\Phi_7 \leq \frac{\epsilon^3}{2} \|\theta_p\|_{l^2(L^2)}^2 + \frac{1}{2\epsilon} \|\eta_{\mathbf{u}t}\|_{l^2(L^2)}^2 + \frac{\Delta t^2}{2\epsilon} \int_0^{t_N} \|\eta_{\mathbf{u}tt}\|_{0,\Omega}^2 ds + \frac{1}{2\epsilon} \|\eta_{\mathbf{z}}\|_{l^2(L^2)}^2. \quad (64)$$

We can now combine the individual bounds (58), (59), (60), (61), (62), (63), and (64), with (57) to obtain from (56),

$$\begin{aligned} & \left(\frac{C_k}{2} - \frac{C_c \epsilon}{2} \right) \|\theta_{\mathbf{u}}^N\|_{1,\Omega}^2 + \frac{1}{2} \|\theta_p^N\|_{J,\Omega}^2 + \lambda_{max}^{-1} \|\theta_{\mathbf{z}}\|_{l^2(L^2)}^2 + (1 - C\epsilon) \|\theta_p\|_{l^2(L^2)}^2 \\ & \leq C_c \left(\frac{1}{2\epsilon} + \epsilon \right) \|\theta_{\mathbf{u}}\|_{l^2(H^1)}^2 + \left(\epsilon + \frac{\epsilon}{2} + \frac{1}{4\epsilon} \right) \|\theta_p\|_{l^2(J)}^2 + \frac{1}{2\epsilon} \|\eta_{p_t}\|_{l^2(J)}^2 \\ & \quad + \frac{1}{2\epsilon} \left((C_c + 1) \|\eta_{\mathbf{u}t}\|_{l^2(H^1)}^2 + C_c \|\eta_{\mathbf{u}}^N\|_{1,\Omega}^2 + \lambda_{min}^{-2} \|\eta_{\mathbf{z}}\|_{l^2(L^2)}^2 + C_c^2 \|\eta_{\mathbf{u}}\|_{l^2(H^1)}^2 \right) \\ & \quad + \frac{\Delta t^2}{2\epsilon} \left(\int_0^{t_N} (C_c + 1) \|\eta_{\mathbf{u}tt}\|_{1,\Omega}^2 ds + \int_0^{t_N} \|\eta_{p_{tt}}\|_{J,\Omega}^2 ds + \int_0^{t_N} \|\nabla \cdot \mathbf{u}_{tt}\|_{0,\Omega}^2 ds + \int_0^{t_N} \|p_{tt}\|_{J,\Omega}^2 ds \right). \end{aligned} \quad (65)$$

Now choosing ϵ sufficiently small, and applying a discrete version of Gronwall's lemma, we get

$$\begin{aligned} \|\theta_{\mathbf{u}}^N\|_{1,\Omega}^2 + \|\theta_p^N\|_{J,\Omega}^2 + \|\theta_{\mathbf{z}}\|_{l^2(L^2)}^2 + \|\theta_p\|_{l^2(L^2)}^2 & \leq C \left(\|\eta_{p_t}\|_{l^2(J)}^2 + \|\eta_{\mathbf{u}}^N\|_{1,\Omega}^2 + \|\eta_{\mathbf{u}t}\|_{l^2(H^1)}^2 + \|\eta_{\mathbf{z}}\|_{l^2(L^2)}^2 \right) \\ & \quad + C\Delta t^2 \left(\|\eta_{\mathbf{u}tt}\|_{L^2(H^1)}^2 + \|\eta_{p_{tt}}\|_{L^2(J)}^2 \right) \\ & \quad + C\Delta t^2 \left(\|\nabla \cdot \mathbf{u}_{tt}\|_{L^2(L^2)}^2 + \|p_{tt}\|_{L^2(J)}^2 \right). \end{aligned}$$

Now applying approximation results for the projection (4.2), the bound (11), and taking the square root on both sides, we have

$$\begin{aligned} \|\theta_{\mathbf{u}}^N\|_{1,\Omega} + \|\theta_p^N\|_{J,\Omega} + \|\theta_{\mathbf{z}}\|_{l^2(L^2)} + \|\theta_p\|_{l^2(L^2)} & \leq Ch \left(\|p_t\|_{l^2(H^1)} + \|\mathbf{u}^N\|_{2,\Omega} + \|\mathbf{u}_t\|_{l^2(H^2)} + \|\mathbf{z}\|_{l^2(H^1)} \right) \\ & \quad + Ch\Delta t \left(\|\mathbf{u}_{tt}\|_{L^2(H^2)} + \|p_{tt}\|_{L^2(H^1)} \right) \\ & \quad + C\Delta t \left(\|\nabla \cdot \mathbf{u}_{tt}\|_{L^2(L^2)} + \|p_{tt}\|_{L^2(L^2)} \right). \end{aligned}$$

Because the above holds for all time steps $n = 0, 1, \dots, N$, we can get the desired l^∞ bounds to complete the proof of the theorem. \square

4.4 Auxiliary error estimate on the divergence of the flux

We now present an a-priori auxillary error estimate of the fluid flux, in its natural $Hdiv$ norm.

Lemma 4.4. *Assume that the true solution $(\mathbf{u}, \mathbf{z}, p)$ is in $H^2 \left([H^2(\Omega)]^d \right) \times H^1 \left([H^2(\Omega)]^d \right) \cap H^2 \left([H^1(\Omega)]^d \right) \times H^2 \left(H^1(\Omega) \cap \mathcal{L}(\Omega) \right)$, then the finite element solution (9) satisfies the auxillary error estimate*

$$\begin{aligned} \|\nabla \cdot \theta_{\mathbf{z}}\|_{l^2(L^2)} & \leq Ch \left(\|\mathbf{u}_t\|_{l^2(H^2)} + \|\nabla \cdot \mathbf{z}\|_{l^2(H^1)} + \|\mathbf{z}_t\|_{l^2(H^1)} + \|p_t\|_{l^2(H^1)} \right) \\ & \quad + Ch\Delta t \left(\|\nabla \cdot \mathbf{u}_{tt}\|_{L^2(H^1)} + \|\mathbf{z}_{tt}\|_{L^2(H^1)} + \|p_{tt}\|_{L^2(H^1)} \right) \\ & \quad + C\Delta t \left(\|p_{tt}\|_{L^2(L^2)} + \|\nabla \cdot \mathbf{u}_{tt}\|_{L^2(L^2)} \right). \end{aligned}$$

Proof. This proof is very similar to the previous proof. We will therefore only show the main intermediate results. We can get the following Galerkin orthogonality by subtracting the fully-discrete weak formulation (9) from the continuous formulation (6),

$$a(\mathbf{u}(t_n) - \mathbf{u}_h^n, \mathbf{v}_h) - (p(t_n) - p_h^n, \nabla \cdot \mathbf{v}_h) = 0 \quad \forall \mathbf{v}_h \in \mathbf{W}_{h0}^E, \quad (66a)$$

$$(\kappa^{-1}(\mathbf{z}(t_n) - \mathbf{z}_h^n), \mathbf{w}_h) - (p(t_n) - p_h^n, \nabla \cdot \mathbf{w}_h) = 0 \quad \forall \mathbf{w}_h \in \mathbf{W}_{h0}^D, \quad (66b)$$

$$(\nabla \cdot (\mathbf{u}_{\delta t}(t_n) - \mathbf{u}_{\delta t,h}^n) + \nabla \cdot (\mathbf{z}(t_n) - \mathbf{z}_h^n), q_h) + J(p(t_n) - p_{\delta t,h}^n, q_h) = (\nabla \cdot \rho_{\mathbf{u}}^n, q_h) + J(\rho_p^n, q_h) \quad \forall q_h \in Q_h. \quad (66c)$$

Note that this also holds at the previous time step such that

$$a(\mathbf{u}(t_{n-1}) - \mathbf{u}_h^{n-1}, \mathbf{v}_h) - (p(t_{n-1}) - p_h^{n-1}, \nabla \cdot \mathbf{v}_h) = 0 \quad \forall \mathbf{v}_h \in \mathbf{W}_{h0}^E, \quad (67a)$$

$$(\kappa^{-1}(\mathbf{z}(t_{n-1}) - \mathbf{z}_h^{n-1}), \mathbf{w}_h) - (p(t_{n-1}) - p_h^{n-1}, \nabla \cdot \mathbf{w}_h) = 0 \quad \forall \mathbf{w}_h \in \mathbf{W}_{h0}^D. \quad (67b)$$

Subtracting (67a) from (66a) and dividing by Δt , and performing a similar operation for (67b) and (66b), we obtain

$$a(\mathbf{u}_{\delta t}(t_n) - \mathbf{u}_{\delta t,h}^n, \mathbf{v}_h) - (p_{\delta t}(t_n) - p_{\delta t,h}^n, \nabla \cdot \mathbf{v}_h) = 0 \quad \forall \mathbf{v}_h \in \mathbf{W}_{h0}^E, \quad (68a)$$

$$(\kappa^{-1}(\mathbf{z}_{\delta t}(t_n) - \mathbf{z}_{\delta t,h}^n), \mathbf{w}_h) - (p_{\delta t}(t_n) - p_{\delta t,h}^n, \nabla \cdot \mathbf{w}_h) = 0 \quad \forall \mathbf{w}_h \in \mathbf{W}_{h0}^D, \quad (68b)$$

$$(\nabla \cdot (\mathbf{u}_{\delta t}(t_n) - \mathbf{u}_{\delta t,h}^n), q_h) + (\nabla \cdot (\mathbf{z}(t_n) - \mathbf{z}_h^n), q_h) + J(p(t_n) - p_{\delta t,h}^n, q_h) = (\nabla \cdot \rho_{\mathbf{u}}^n, q_h) + J(\rho_p^n, q_h) \quad \forall q_h \in Q_h. \quad (68c)$$

Writing

$$\mathbf{u}_{\delta t}(t_n) - \mathbf{u}_{\delta t,h}^n = (\mathbf{u}_{\delta t}(t_n) - \pi_h \mathbf{u}_{\delta t}(t_n)) + (\pi_h \mathbf{u}_{\delta t}(t_n) - \mathbf{u}_{\delta t,h}^n) = \eta_{\delta t,\mathbf{u}}^n + \theta_{\delta t,\mathbf{u}}^n,$$

and similarly for the other variables. Choosing $\mathbf{v}_h = \beta \theta_{\delta t,\mathbf{u}}^n + \pi_h \mathbf{v}_p$, $\mathbf{w}_h = \beta \theta_{\delta t,\mathbf{z}}^n$, $q_h = \beta \theta_{\delta t,p}^n + \nabla \cdot \theta_{\delta t,\mathbf{z}}^n$, with $\nabla \cdot \mathbf{v}_p = \theta_{\delta t,p}$, adding (68a), (68b) and (68c), rearranging, multiplying by Δt , and summing we have,

$$\sum_{n=1}^N \Delta t \mathcal{B}_h^n[(\theta_{\mathbf{u}}^n + \pi_h \mathbf{v}_p, \theta_{\mathbf{z}}^n, \theta_p^n), (\beta \theta_{\delta t,\mathbf{u}}^n, \beta \theta_{\delta t,\mathbf{z}}^n, \beta \theta_{\delta t,p}^n + \nabla \cdot \theta_{\delta t,\mathbf{z}}^n)] = \Psi_1 + \Psi_2 + \Psi_3 + \Psi_4 + \Psi_5 + \Psi_6 \quad (69)$$

where

$$\begin{aligned} \Psi_1 &= - \sum_{n=1}^N \Delta t a(\eta_{\delta t,\mathbf{u}}^n, \beta \theta_{\delta t,\mathbf{u}}^n + \pi_h \mathbf{v}_p), & \Psi_2 &= - \sum_{n=1}^N \Delta t (\nabla \cdot (\eta_{\delta t,\mathbf{u}}^n + \eta_{\delta t,\mathbf{z}}^n), \nabla \cdot \theta_{\delta t,\mathbf{z}}^n + \beta \theta_{\delta t,p}^n), \\ \Psi_3 &= \sum_{n=1}^N \Delta t J(\eta_{\delta t,p}^n, \nabla \cdot \theta_{\delta t,\mathbf{z}}^n - \beta \theta_{\delta t,p}^n), & \Psi_4 &= - \sum_{n=1}^N \Delta t (\kappa^{-1}(\eta_{\delta t,\mathbf{z}}^n, \beta \theta_{\delta t,\mathbf{z}}^n)), \\ \Psi_5 &= \sum_{n=1}^N \Delta t J(\rho_p^n, \beta \theta_{\delta t,p}^n + \nabla \cdot \theta_{\delta t,\mathbf{z}}^n), & \Psi_6 &= \sum_{n=1}^N \Delta t (\nabla \cdot \rho_{\mathbf{u}}^n, \beta \theta_{\delta t,p}^n + \nabla \cdot \theta_{\delta t,\mathbf{z}}^n). \end{aligned}$$

Using (47), and $\theta_{\mathbf{z}}^0 = 0$, we can immediately bound the left hand side of (69), such that

$$\begin{aligned} & \left(\beta C_k - \frac{C_p + C_c}{2\epsilon} \right) \|\theta_{\delta t, \mathbf{u}}\|_{l^2(H^1)}^2 + \frac{\beta \lambda_{max}^{-1}}{2} \|\theta_{\mathbf{z}}^N\|_{0, \Omega}^2 + \left(\beta - \frac{3}{4\epsilon} \right) \|\theta_{\delta t, p}\|_{l^2(J)}^2 + (1 - \epsilon(1 + c_z)) \|\nabla \cdot \theta_{\mathbf{z}}\|_{l^2(L^2)}^2 \\ & + (1 - C\epsilon) \|\theta_{\delta t, p}\|_{l^2(L^2)}^2 \leq \sum_{n=1}^N \Delta t \mathcal{B}_h^n[(\theta_{\mathbf{u}}^n + \pi_h \mathbf{v}_p, \theta_{\mathbf{z}}^n, \theta_p^n), (\beta \theta_{\delta t, \mathbf{u}}^n, \beta \theta_{\mathbf{z}}^n, \beta \theta_{\delta t, p}^n + \nabla \cdot \theta_{\mathbf{z}}^n)]. \end{aligned} \quad (70)$$

Here we have also assumed that $\theta_{\mathbf{z}}^0 = 0$. We now bound the terms on the right hand side of (69) using machinery developed during previous proofs.

$$\Psi_1 \leq \frac{C_c \epsilon}{2} \|\theta_{\delta t, \mathbf{u}}\|_{l^2(H^1)}^2 + \frac{\hat{c}^2 \epsilon}{2} \|\theta_{\delta t, p}\|_{l^2(L^2)}^2 + \frac{\beta^2 C_c}{\epsilon} \|\eta_{\mathbf{u}_t}\|_{l^2(H^1)}^2 + \frac{\beta^2 C_c \Delta t^2}{\epsilon} \int_0^{t_N} \|\eta_{\mathbf{u}_{tt}}\|_{1, \Omega}^2 ds, \quad (71)$$

$$\begin{aligned} \Psi_2 & \leq \frac{1 + \beta^2}{2\epsilon} \|\nabla \cdot \eta_{\mathbf{z}}\|_{l^2(L^2)}^2 + \epsilon \|\nabla \cdot \theta_{\mathbf{z}}\|_{l^2(L^2)}^2 + \epsilon \|\theta_{\delta t, p}\|_{l^2(L^2)}^2 \\ & + \frac{1 + \beta^2}{2\epsilon} \|\nabla \cdot \eta_{\mathbf{u}_t}\|_{l^2(L^2)}^2 + \frac{\Delta t^2 (1 + \beta^2)}{2\epsilon} \int_0^{t_N} \|\nabla \cdot \eta_{\mathbf{u}_{tt}}\|_{0, \Omega}^2 ds, \end{aligned} \quad (72)$$

$$\begin{aligned} \Psi_3 & \leq \epsilon c_z \|\nabla \cdot \theta_{\mathbf{z}}\|_{l^2(L^2)}^2 + \frac{\epsilon}{2} \|\theta_{\delta t, p}^n\|_{l^2(J)}^2 \\ & + \frac{1 + \beta^2}{2\epsilon} \|\eta_{p_t}\|_{l^2(J)}^2 + \frac{(1 + \beta^2) \Delta t^2}{2\epsilon} \int_0^{t_N} \|\eta_{p_{tt}}\|_{J, \Omega}^2 ds, \end{aligned} \quad (73)$$

$$\Psi_4 \leq \frac{\epsilon}{2} \|\theta_{\mathbf{z}}\|_{l^2(L^2)}^2 + \frac{\lambda_{min}^{-2} \beta^2}{2\epsilon} \left(\|\eta_{\mathbf{z}_t}\|_{l^2(L^2)}^2 + \Delta t^2 \int_0^{t_N} \|\eta_{\mathbf{z}_{tt}}\|_{0, \Omega}^2 ds \right), \quad (74)$$

$$\Psi_5 \leq \frac{\epsilon}{2} \|\theta_{\delta t, p}\|_{l^2(J)}^2 + \epsilon c_z \|\nabla \cdot \theta_{\mathbf{z}}\|_{l^2(L^2)}^2 + \frac{(1 + \beta^2) \Delta t^2}{2\epsilon} \int_0^{t_N} \|p_{tt}\|_{J, \Omega}^2 ds, \quad (75)$$

$$\Psi_6 \leq \frac{\epsilon}{2} \|\theta_{\delta t, p}\|_{l^2(L^2)}^2 + \frac{\epsilon}{2} \|\nabla \cdot \theta_{\mathbf{z}}\|_{l^2(L^2)}^2 + \frac{(1 + \beta^2) \Delta t^2}{2\epsilon} \int_0^{t_N} \|\nabla \cdot \mathbf{u}_{tt}\|_{0, \Omega}^2 ds. \quad (76)$$

We can now combine the individual bounds (71), (72), (73), (74), and (75), with (70) to obtain from (69),

$$\begin{aligned} & \left(\beta C_k - \frac{C_p}{2\epsilon} - \frac{C_c \epsilon}{2} \right) \|\theta_{\delta t, \mathbf{u}}\|_{l^2(H^1)}^2 + \frac{\lambda_{max}^{-1} \beta}{2} \|\theta_{\mathbf{z}}^N\|_{0, \Omega}^2 + \left(1 - 3\epsilon(c_z + \frac{1}{2}) \right) \|\nabla \cdot \theta_{\mathbf{z}}\|_{l^2(L^2)}^2 \\ & + \left(\beta - \frac{1}{2\epsilon} - \frac{3\epsilon}{2} \right) \|\theta_{\delta t, p}\|_{l^2(J)}^2 + \left(1 - \epsilon(C + \frac{\hat{c}^2}{2} + 1) \right) \|\theta_{\delta t, p}\|_{l^2(L^2)}^2 \leq \frac{\epsilon}{2} \|\theta_{\mathbf{z}}\|_{l^2(L^2)}^2 + \left(\frac{1 + \beta^2}{2\epsilon} + \frac{\beta^2 C_c}{\epsilon} \right) \|\eta_{\mathbf{u}_t}\|_{l^2(H^1)}^2 \\ & + \frac{1 + \beta^2}{2\epsilon} \|\nabla \cdot \eta_{\mathbf{z}}\|_{l^2(L^2)}^2 + \frac{\lambda_{min}^{-2} \beta^2}{2\epsilon} \|\nabla \cdot \eta_{\mathbf{z}_t}\|_{l^2(L^2)}^2 + \frac{1 + \beta^2}{2\epsilon} \|\eta_{p_t}\|_{l^2(J)}^2 + \left(\frac{1 + \beta^2}{2\epsilon} + \frac{\beta^2 C_c}{\epsilon} \right) \Delta t^2 \|\eta_{\mathbf{u}_{tt}}\|_{L^2(H^1)}^2 \\ & + \frac{\lambda_{min}^{-2} \beta^2 \Delta t^2}{2\epsilon} \|\eta_{\mathbf{z}_{tt}}\|_{L^2(L^2)}^2 + \frac{(1 + \beta^2) \Delta t^2}{2\epsilon} \left(\|\eta_{p_{tt}}\|_{L^2(J)}^2 + \|p_{tt}\|_{L^2(J)}^2 + \|\nabla \cdot \mathbf{u}_{tt}\|_{L^2(L^2)}^2 \right). \end{aligned}$$

Now choosing ϵ sufficiently small, $\beta \geq \max \left[\frac{C_p}{\epsilon C_k} + \frac{C_c \epsilon}{2C_k}, \frac{1}{2\epsilon} + \frac{3\epsilon}{2} \right]$, and applying a discrete version of Gronwall's lemma, we get

$$\begin{aligned} & \|\theta_{\delta t, \mathbf{u}}\|_{l^2(H^1)}^2 + \|\theta_{\mathbf{z}}^N\|_{0, \Omega}^2 + \|\nabla \cdot \theta_{\mathbf{z}}\|_{l^2(L^2)}^2 + \|\theta_{\delta t, p}\|_{l^2(J)}^2 + \|\theta_{\delta t, p}\|_{l^2(L^2)}^2 \\ & \leq C \left(\|\eta_{\mathbf{u}_t}\|_{l^2(H^1)}^2 + \|\nabla \cdot \eta_{\mathbf{z}}\|_{l^2(L^2)}^2 + \|\nabla \cdot \eta_{\mathbf{z}_t}\|_{l^2(L^2)}^2 + \|\eta_{p_t}\|_{l^2(J)}^2 + \|\eta_{\mathbf{z}}\|_{l^2(L^2)}^2 \right) \\ & \quad + C\Delta t^2 \left(\|\nabla \cdot \eta_{\mathbf{u}_{tt}}\|_{L^2(L^2)}^2 + \|\eta_{\mathbf{z}_{tt}}\|_{L^2(L^2)}^2 + \|\eta_{p_{tt}}\|_{L^2(J)}^2 \right) + C\Delta t^2 \left(\|p_{tt}\|_{L^2(J)}^2 + \|\nabla \cdot \mathbf{u}_{tt}\|_{L^2(J)}^2 \right). \end{aligned}$$

Applying standard approximation results, using the bound (11), and noting that $\|\theta_{\delta t, \mathbf{u}}\|_{l^2(H^1)}^2, \|\theta_{\mathbf{z}}\|_{l^2(L^2)}^2, \|\theta_{\delta t, p}\|_{l^2(J)}^2, \|\theta_{\delta t, p}\|_{l^2(L^2)}^2 \geq 0$, we are left with

$$\begin{aligned} \|\nabla \cdot \theta_{\mathbf{z}}^n\|_{l^2(L^2)}^2 & \leq Ch^2 \left(\|\mathbf{u}_t\|_{l^2(H^2)}^2 + \|\nabla \cdot \mathbf{z}\|_{l^2(H^1)}^2 + \|\nabla \cdot \mathbf{z}_t\|_{l^2(H^1)}^2 + \|p_t\|_{l^2(H^1)}^2 + \|\mathbf{z}\|_{l^2(H^1)}^2 \right) \\ & \quad + Ch^2\Delta t^2 \left(\|\nabla \cdot \mathbf{u}_{tt}\|_{L^2(H^1)}^2 + \|\mathbf{z}_{tt}\|_{L^2(H^1)}^2 + \|p_{tt}\|_{L^2(H^1)}^2 \right) \\ & \quad + C\Delta t^2 \left(\|p_{tt}\|_{L^2(J)}^2 + \|\nabla \cdot \mathbf{u}_{tt}\|_{L^2(J)}^2 \right). \end{aligned}$$

Taking the square root on both sides completes the proof. \square

Theorem 4.5. *Assume that the true solution $(\mathbf{u}, \mathbf{z}, p)$ is in $H^2 \left([H^2(\Omega)]^d \right) \times H^1 \left([H^2(\Omega)]^d \right) \cap H^2 \left([H^1(\Omega)]^d \right) \times H^2 \left(H^1(\Omega) \cap \mathcal{L}(\Omega) \right)$, then the finite element solution (9) satisfies the error estimate*

$$\|\mathbf{u} - \mathbf{u}_h\|_{l^\infty(H^1)} + \|\nabla \cdot (\mathbf{z} - \mathbf{z}_h)\|_{l^2(L^2)} + \|\mathbf{z} - \mathbf{z}_h\|_{l^2(L^2)} + \|p - p_h\|_{l^\infty(L^2)} \leq C(h + \Delta t).$$

Proof. We first write the errors as $\mathbf{u}^n - \mathbf{u}_h^n = (\mathbf{u}^n - \pi_h \mathbf{u}^n) + (\pi_h \mathbf{u}^n - \mathbf{u}_h^n) = \eta_{\mathbf{u}}^n + \theta_{\mathbf{u}}^n$, and similarly for the other variables. Using lemma 4.2 we can bound the interpolation errors, and using lemma 4.3 and lemma 4.4 we can bound the auxillary errors to give the desired result. \square

5 Numerical Results

In this section, we present both two-dimensional and three-dimensional numerical experiments with analytical solutions to verify the theoretical convergence rates of the fully-discrete finite element method developed in this paper. We also test our method on the popular 2D cantilever bracket problem to make sure our method is able to overcome the spurious pressure oscillations often experienced in poroelastic simulations. Finally, a 3D unconfined compression problem is presented that highlights the added mass effect of the method for different choices of the stabilization parameter δ .

5.1 Implementation

For the implementation we used the C++ library libmesh [Kirk et al., 2006], and the multi-frontal direct solver mumps [Amestoy et al., 2000] to solve the resulting linear system. To solve the full

Biot model problem (1), we need to solve the following linear system at each time step:

$$\begin{bmatrix} \mathbf{A} & 0 & \alpha \mathbf{B}^T \\ 0 & \mathbf{M} & \mathbf{B}^T \\ \alpha \mathbf{B} & \Delta t \mathbf{B} & c_0 \mathbf{Q} + \mathbf{J} \end{bmatrix} \begin{bmatrix} \mathbf{u}^n \\ \mathbf{z}^n \\ \mathbf{p}^n \end{bmatrix} = \begin{bmatrix} \mathbf{f} \\ \mathbf{b} \\ \Delta t q + \mathbf{B} \mathbf{u}^{n-1} + c_0 \mathbf{Q} \mathbf{p}^{n-1} + \mathbf{J} \mathbf{p}^{n-1} \end{bmatrix},$$

where we have defined the following matrices:

$$\mathbf{A} = [\mathbf{a}_{ij}], \quad \mathbf{a}_{ij} = \int_{\Omega} 2\mu_s \nabla \phi_i : \nabla \phi_j + \lambda (\nabla \cdot \phi_i)(\nabla \cdot \phi_j),$$

$$\mathbf{M} = [\mathbf{m}_{ij}], \quad \mathbf{m}_{ij} = \int_{\Omega} \kappa^{-1} \phi_i \cdot \phi_j,$$

$$\mathbf{B} = [\mathbf{b}_{ij}], \quad \mathbf{b}_{ij} = - \int_{\Omega} \psi_i \nabla \cdot \phi_j,$$

$$\mathbf{Q} = [\mathbf{q}_{ij}], \quad \mathbf{q}_{ij} = \int_{\Omega} \psi_i \cdot \psi_j,$$

$$\mathbf{J} = [\mathbf{j}_{ij}], \quad \mathbf{j}_{ij} = \delta \sum_K \int_{\partial K \setminus \partial \Omega} h_{\partial K} [\psi_i] [\psi_j] \, ds.$$

Here ϕ_i are vector valued linear basis functions such that the displacement vector can be written as $\mathbf{u}^n = \sum_{i=1}^{n_u} \mathbf{u}_i^n \phi_i$, with $\sum_{i=1}^{n_u} \mathbf{u}_i^n \phi_i \in \mathbf{W}_h^E$. Similarly for the relative fluid vector we have $\mathbf{z}^n = \sum_{i=1}^{n_z} \mathbf{z}_i^n \phi_i$, with $\sum_{i=1}^{n_z} \mathbf{z}_i^n \phi_i \in \mathbf{W}_h^D$. The scalar valued constant basis functions ψ_i are used to approximate the pressure, such that $\mathbf{p}^n = \sum_{i=1}^{n_p} p_i^n \psi_i$, with $\sum_{i=1}^{n_p} p_i^n \psi_i \in Q_h$.

5.2 2D convergence study

We adapt a test problem used in Burman and Hansbo [2007] to verify the convergence of our method. To simplify the analytical solution we chose parameters so that the equilibrium equations are simplified as below, yet retain all the analytical properties and difficulties of the original problem. Any conclusions drawn from this convergence study therefore also apply to the original system of equations (1). The analytical solution of the pressure is given by $p = \sin(2\pi x) \sin(2\pi y) \sin(2\pi t)$, with $t \in [0, 0.25]$. For this test problem the domain, Ω , is the unit square, with boundary $\partial \Omega = \Gamma_d$ for the mixture, and $\partial \Omega = \Gamma_f$ for the fluid. The simplified system of equations is given by

$$-\nabla^2 \mathbf{u} + \nabla p = 0 \quad \text{in } \Omega, \tag{77a}$$

$$\mathbf{z} + \nabla p = 0 \quad \text{in } \Omega, \tag{77b}$$

$$\nabla \cdot (\mathbf{u}_t + \mathbf{z}) = g \quad \text{in } \Omega, \tag{77c}$$

$$\mathbf{u}(t) = \mathbf{u}_D \quad \text{on } \Gamma_d, \tag{77d}$$

$$\mathbf{z}(t) \cdot \mathbf{n} = q_D \quad \text{on } \Gamma_f, \tag{77e}$$

$$\mathbf{u}(0) = 0 \quad \text{in } \Omega, \tag{77f}$$

where the displacement boundary condition, the fluid flux boundary condition, and the source term are calculated to be

$$\mathbf{u}_D = \begin{pmatrix} -\frac{1}{4}\pi \cos(2\pi x) \sin(2\pi y) \sin(2\pi t) \\ -\frac{1}{4}\pi \sin(2\pi x) \cos(2\pi y) \sin(2\pi t) \end{pmatrix},$$

$$q_D = \begin{pmatrix} -2\pi \cos(2\pi x) \sin(2\pi y) \sin(2\pi t) \\ -2\pi \sin(2\pi x) \cos(2\pi y) \sin(2\pi t) \end{pmatrix} \cdot \mathbf{n},$$

$$g = 2\pi \sin(2\pi x) \sin(2\pi y) \cos(2\pi t) + 8\pi^2 \sin(2\pi x) \sin(2\pi y) \sin(2\pi t).$$

Figure 1a illustrates what happens when the stabilization parameter δ is not chosen large enough ($\delta = 0.1$), resulting in a spurious pressure solution. For this test problem we have found that a value of $\delta = 1$ is sufficiently large to result in a smooth pressure solution (see Figure 1b). The value of δ required to produce a stable solution depends on the geometry and material parameters of the particular problem under investigation, but is independent of any mesh parameters. In Figure 2, we show the convergence of the method in relevant norms for each variable, with $\delta = 1, 10, 100$. The rates of convergence agree with the theoretically derived error estimates. Figure 3 and Figure 4 show the deformation, pressure, and fluid flux in the x and y directions at time $t = 0.125$ and $t = 0.25$, respectively.

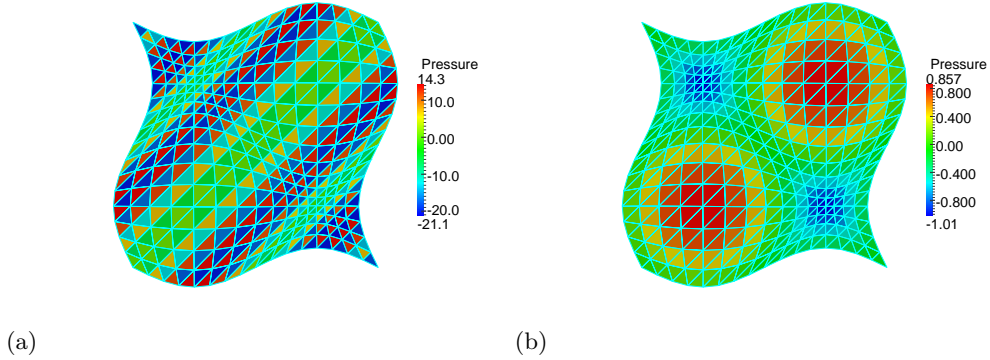


Figure 1: (a) Unstable pressure field, caused by not choosing the stabilization parameter δ large enough, with $\delta = 0.1$, at $t = 0.25$. (b) Stable pressure field, with $\delta = 1$ at $t = 0.25$.

5.3 3D convergence study

We extend the previous test problem to a unit cube. We now set the analytical pressure to $p = \sin(2\pi x) \sin(2\pi y) \sin(2\pi z) \sin(2\pi t)$, which gives the following displacement boundary condition, fluid flux boundary condition, and right hand side source term

$$\mathbf{u}_D = \begin{pmatrix} -\frac{1}{6}\pi \cos(2\pi x) \sin(2\pi y) \sin(2\pi z) \sin(2\pi t) \\ -\frac{1}{6}\pi \sin(2\pi x) \cos(2\pi y) \sin(2\pi z) \sin(2\pi t) \\ -\frac{1}{6}\pi \sin(2\pi x) \sin(2\pi y) \cos(2\pi z) \sin(2\pi t) \end{pmatrix},$$

$$q_d = \begin{pmatrix} -2\pi \cos(2\pi x) \sin(2\pi y) \sin(2\pi z) \sin(2\pi t) \\ -2\pi \sin(2\pi x) \cos(2\pi y) \sin(2\pi z) \sin(2\pi t) \\ -2\pi \sin(2\pi x) \sin(2\pi y) \cos(2\pi z) \sin(2\pi t) \end{pmatrix} \cdot \mathbf{n},$$

$$g = 2\pi \sin(2\pi x) \sin(2\pi y) \sin(2\pi z) \cos(2\pi t) + 12\pi^2 \sin(2\pi x) \sin(2\pi y) \sin(2\pi z) \sin(2\pi t).$$

In Figure 5, we show the 3D convergence of the method in relevant norms for each variable, with $\delta = 0.001, 0.01, 0.1$. The rates of convergence agree with the theoretically derived error estimates.

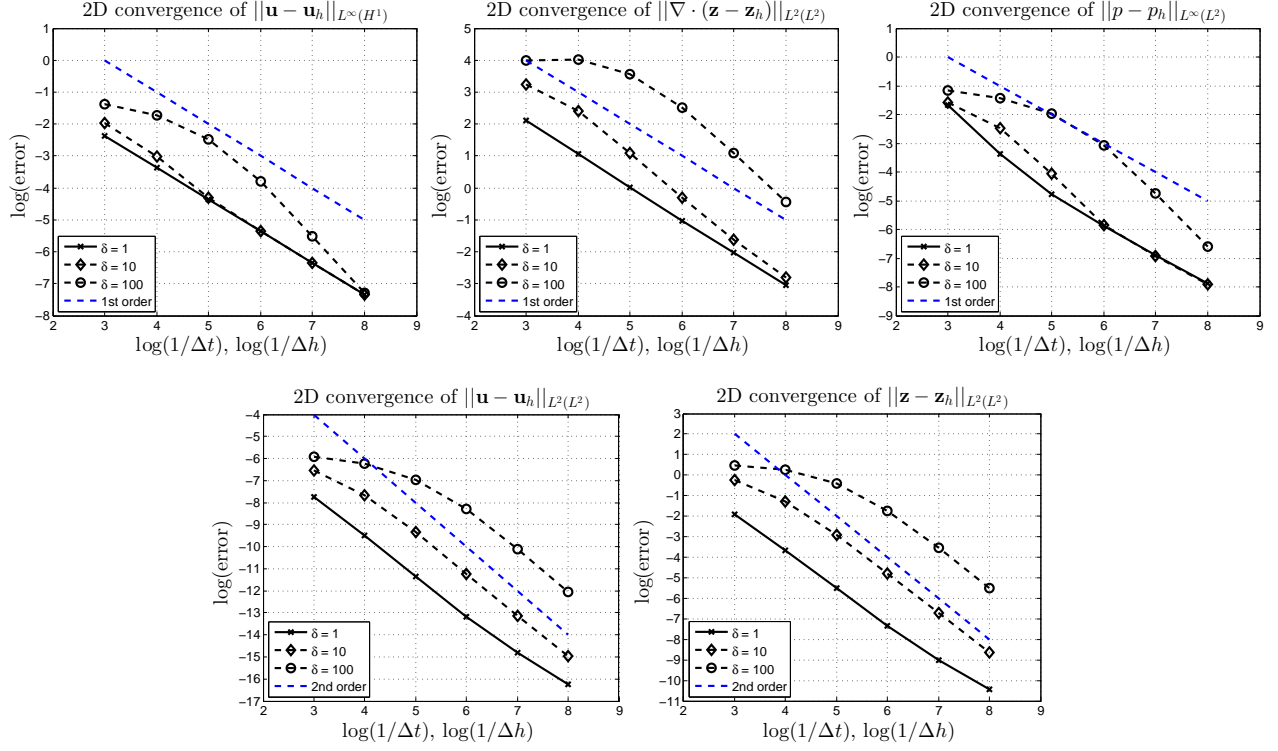


Figure 2: Convergence of the displacement, fluid flux, and pressure errors in their respective norms of the simplified poroelastic 2D test problem with different (stable) values for the stabilization parameter δ .

We have observed that for 3D problems δ can be chosen to be very small compared to 2D problems, making the effect of the stabilization term negligible to the system. This can be explained by the improved ratio of solid displacement and fluid flux nodes to pressure nodes in 3 dimensions, easing the LBB condition, the violation of which explains the spurious pressure oscillations found in unstable finite element formulations.

5.4 2D cantilever bracket problem

It has been shown in Phillips and Wheeler [2009] that continuous Galerkin methods (CG/mixed) developed in Phillips and Wheeler [2007a,b] are susceptible to spurious pressure oscillations. The cause of this pressure instability has been attributed to a phenomenon called ‘locking’ by Phillips and Wheeler [2009], who give a discussion of locking in poroelasticity and show how it relates to the locking phenomenon found in plane linear elasticity problems. A more recent paper by Haga et al. [2012] also investigates the cause of these pressure oscillations, they suggest that for low permeabilities the pressure oscillations are caused by a violation of the inf-sup (LBB) condition. Various methods which approximate the displacement using discontinuous and nonconforming elements have been proposed to overcome this problem [see, e.g., Li and Li, 2012; Liu, 2004; Phillips and Wheeler, 2008; Yi, 2013].

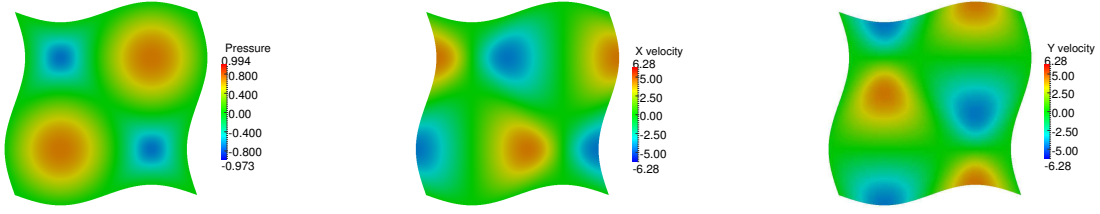


Figure 3: Pressure (left), x -fluid flux (middle), and y -fluid flux (right) at $t = 0.125$.

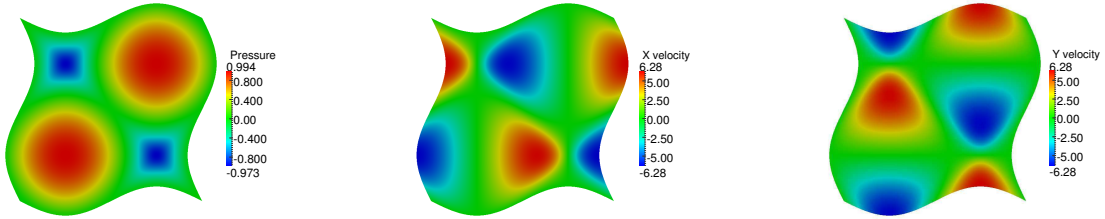


Figure 4: Pressure (left), x -fluid flux (right), and y -fluid flux (middle) at $t = 0.25$.

In this example, we consider the 2D cantilever bracket problem. The same test problem has also been used in Phillips and Wheeler [2009] to showcase the problem of spurious pressure oscillation, and used in Liu [2004] and Yi [2013] to demonstrate that their method is able to overcome these spurious pressure oscillations. The cantilever bracket problem (shown in Figure 6a) is solved on a unit square $[0, 1]^2$. No-flow flux boundary conditions are applied along all sides, the deformation is fixed ($\mathbf{u} = 0$) along the left hand-side ($x = 0$), and a downward traction force is applied along the top edge ($y = 1$). The right and bottom sides are traction-free. For this numerical experiment, we set $\Delta t = 0.001$, $h = 1/96$, $\delta = 5e - 6$, and choose the same material parameters as in Phillips and Wheeler [2009] that typically cause locking: $E = 1e + 5$, $\nu = 0.4$, $\alpha = 0.93$, $c_0 = 0$, $\kappa = 1e - 7$. The proposed stabilized finite element method yields a smooth pressure solution without any oscillations as is shown in Figure 6b.

5.5 3D unconfined compression stress relaxation

In this test, a cylindrical specimen of porous tissue is exposed to a prescribed displacement in the axial direction while left free to expand radially. The original experiment involved a specimen of articular cartilage being compressed via impervious smooth plates as shown in Figure 7a, note that the two plates are not explicitly modelled in the simulation, but are realised through displacement boundary conditions. After loading the tissue, the displacement is held constant while the tissue under the displacement relaxes in the radial direction due to interstitial fluid flow through the material and the frictionless plates. For the porous tissue, the outer radial boundary is permeable and free-draining, the upper and lower fluid boundaries are impermeable and have a no flux condition imposed. The outer radius and height of the cylinder is $5mm$, whereas the axial compression is

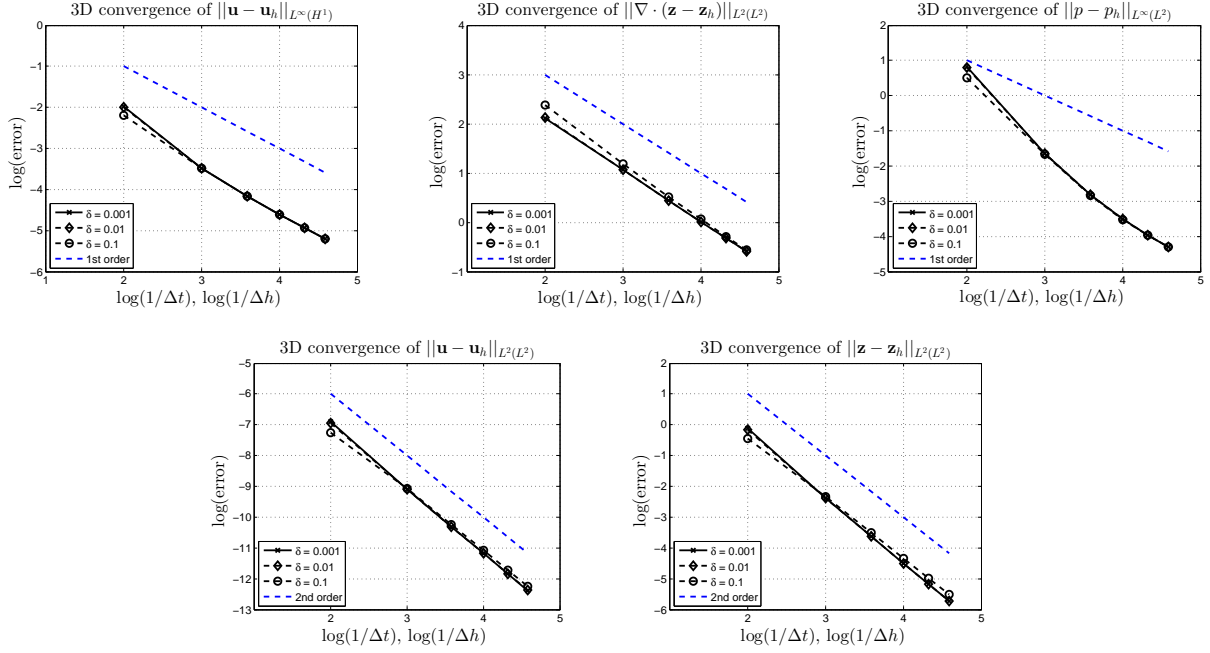


Figure 5: Convergence of the displacement, fluid flux, and pressure errors in their respective norms of the simplified poroelastic 3D test problem with different (stable) values for the stabilization parameter δ .

$\epsilon_0 = 0.01mm$. The bottom of the tissue is constrained in the vertical direction. The fluid pressure was constrained to zero at the outer radial surface. The parameters used for the simulation can be found in Table 2. The material parameters μ_s and λ can be related to the more familiar Young's modulus E and the Poisson ratio ν by $\mu_s = \frac{E}{2(1+\nu)}$ and $\lambda = \frac{E\nu}{(1+\nu)(1-2\nu)}$. For the special case of a cylindrical geometry and assumptions regarding the direction of the fluid flow, Armstrong et al. [1984] found a closed-form analytical solution for the radial displacement on the porous medium in response to a step loading function.

Parameter	Description	Value
κ	Dynamic permeability	$10^{-1} \text{ m}^3 \text{ s kg}^{-1}$
ν	Poisson ratio	0.15
E	Young's modulus	$1000 \text{ kg m}^{-1} \text{ s}^{-2}$
Δt	Time step used in the simulation	0.1 s
T	Final time of the simulation	10 s

Table 2: Parameters used for the unconfined compression test problem.

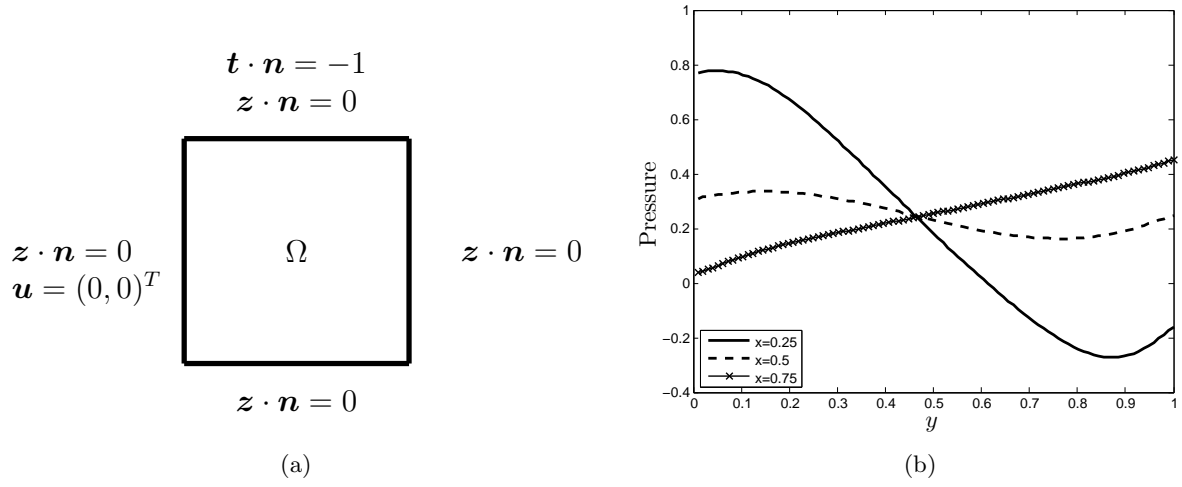


Figure 6: (a) Boundary conditions for the cantilever bracket problem. (b) Pressure solution of the cantilever bracket problem at $t = 0.005$.

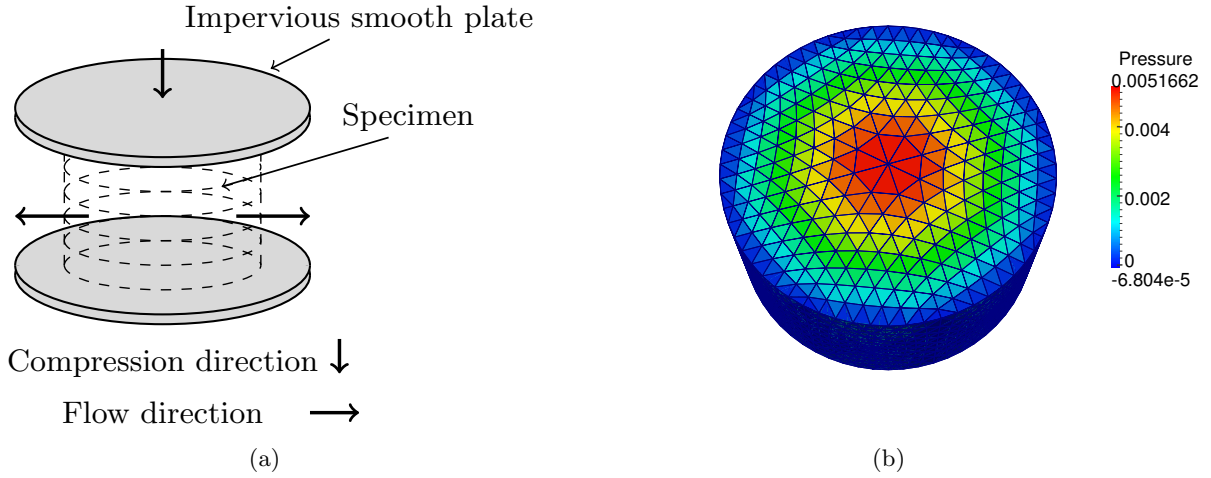


Figure 7: (a) Sketch of the test problem. The porous medium is being compressed between two smooth impervious plates. The frictionless plates permit the porous medium to expand in order to conserve volume and then to gradually relax as the fluid seeps out radially. (b) Pressure field solution at $t = 5s$, using a mesh with 1227 tetrahedra.

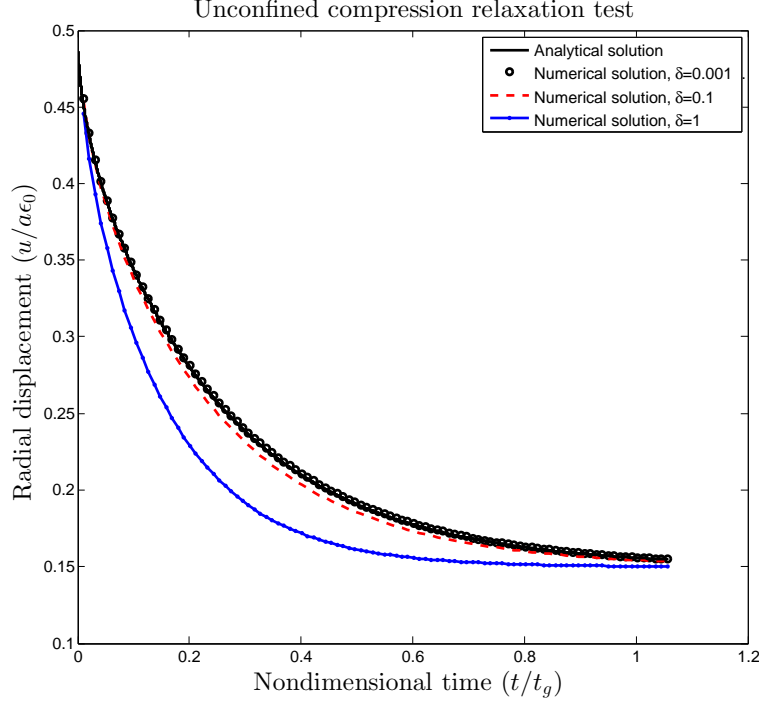


Figure 8: Normalized radial displacement versus normalized time calculated using the analytical solution, and using the proposed numerical method with different values of δ . At $t = 0$ the radial expansion is half of the axial compression indicating the instantaneous incompressibility of the poroelastic tissue. The final amount of tissue recoil depends on the intrinsic Poisson ratio of the tissue skeleton.

The analytical solution for the radial displacement to this unconfined compression test is given by

$$\frac{u}{a}(a, t) = \epsilon_0 \left[\nu + (1 - 2\nu)(1 - \nu) \sum_{n=1}^{\infty} \frac{\exp(-\alpha_n^2 \frac{H_A k t}{a^2})}{\alpha_n^2 (1 - \nu)^2 - (1 - \nu)} \right]. \quad (78)$$

Here α_n are the solutions to the characteristic equation, given by $J_1(x) - (1 - \nu)xJ_0(x)/(1 - 2\nu) = 0$, where J_0 and J_1 are Bessel functions. We also have that ϵ_0 is the amplitude of the applied axial strain, a is the radius of the cylinder, and t_g is the characteristic time of diffusion (relaxation) given by $t_g = a^2/Hk$, where $H = \lambda + 2\mu_s$ is the aggregate modulus of the elastic solid skeleton, and k is the permeability. The radial displacement predicted by our implementation (Figure 8) using a small value of $\delta = 0.001$ gives a root mean squared error of 6.7×10^{-4} against the analytical solution provided by Armstrong et al. [1984], and yields a stable solution. The same test problem has also been used to verify other poroelastic software such as FEBio [Maas et al., 2012]. The analytical solution available for this test problem describes the displacement of the outer radius which is directly dependent on the amount of mass in the system since the porous medium is assumed to be incompressible and fully saturated. It is therefore an ideal test problem for analyzing the effect that the added stabilization term has on the conservation of mass. In Figure 8 we can see that for large values of δ the numerical solution loses mass faster and comes to a steady state that has less mass than the analytical solution. This is a clear limitation of the method and the stability

parameter therefore needs to be chosen carefully. However, for 3D problems δ can be chosen to be very small so this effect is negligible, as can be seen in Figure 8 for a stable value of $\delta = 0.001$.

6 Conclusion

The main contribution of this paper has been to extend the local pressure jump stabilization method [Burman and Hansbo, 2007], commonly used to solve the Stokes or Darcy equations using piecewise linear approximations for the velocities, and piecewise constant approximations for pressure variable, to three-field poroelasticity. We have presented a stability result for the discretized equations that guarantees the existence of a unique solution of the resulting linear system at each time step, and derived an energy estimate which can be used to prove weak convergence of the discretized system to the continuous problem as the mesh parameters tend to zero. We also derived an optimal error estimate which includes an error for the fluid flux in its natural $Hdiv$ norm. To our knowledge no previous papers have been able to show convergence of a finite element method solving the three-field poroelastic equations in this norm. For practical purposes we have also given a description of the implementation, along with numerical experiments in 2D and 3D that illustrate the convergence of the method, show the effectiveness of the method to overcome spurious pressure oscillations, and evaluate the added mass effect of the stabilization term.

References

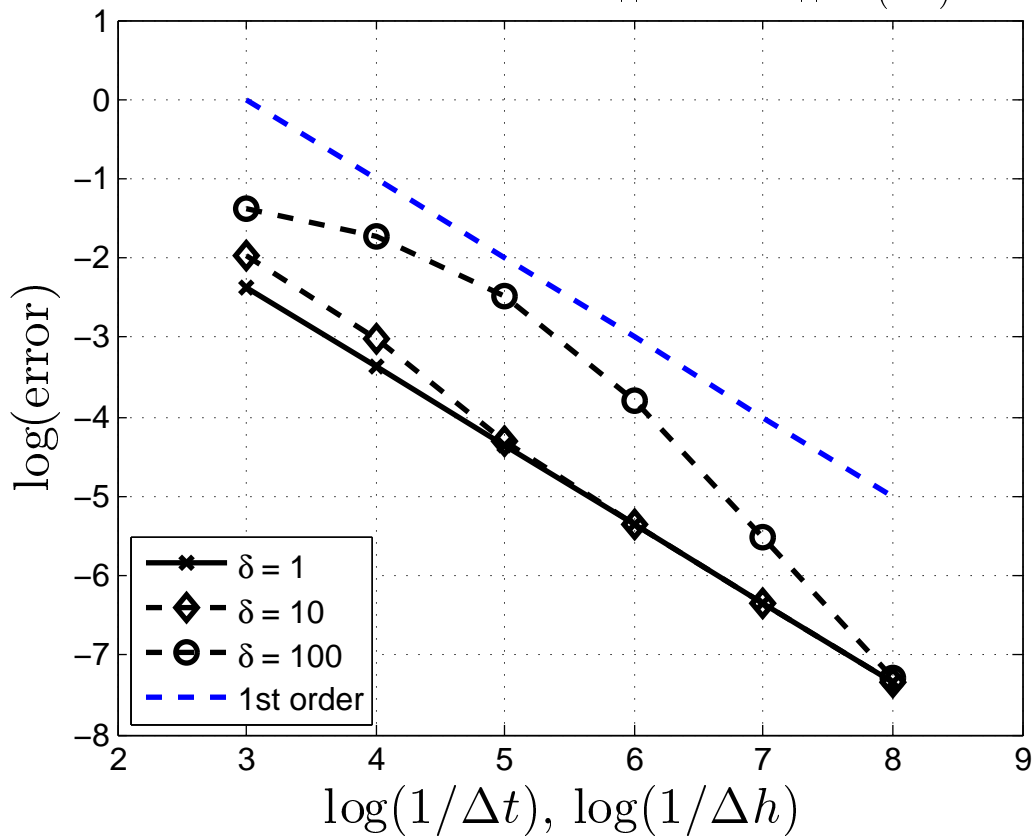
- Patrick R Amestoy, Iain S Duff, and J L'Excellent. Multifrontal parallel distributed symmetric and unsymmetric solvers. *Computer methods in applied mechanics and engineering*, 184(2):501–520, 2000.
- C.G Armstrong, W.M Lai, and V.C Mow. An analysis of the unconfined compression of articular cartilage. *Journal of Biomechanical Engineering*, 106:73–165, 1984.
- Ivo Babuška. Error-bounds for finite element method. *Numerische Mathematik*, 16(4):322–333, 1971.
- S. Badia, A. Quaini, and A. Quarteroni. Coupling Biot and Navier-Stokes equations for modelling fluid-poroelastic media interaction. *Journal of Computational Physics*, 228(21):7986–8014, 2009.
- Hélène Barucq, Monique Madaune-Tort, and Patrick Saint-Macary. Some existence-uniqueness results for a class of one-dimensional nonlinear Biot models. *Nonlinear Analysis: Theory, Methods & Applications*, 61(4):591–612, 2005.
- P.B. Bochev and C.R. Dohrmann. A computational study of stabilized, low-order C0 finite element approximations of Darcy equations. *Computational Mechanics*, 38(4):323–333, 2006.
- Reint Boer. *Trends in continuum mechanics of porous media*, volume 18. Springer, 2005.
- Susanne C Brenner and Larkin Ridgway Scott. *The mathematical theory of finite element methods*, volume 15. Springer, 2008.
- Erik Burman and Peter Hansbo. A unified stabilized method for Stokes' and Darcy's equations. *Journal of Computational and Applied Mathematics*, 198(1):35–51, 2007.

- V. Carey, D. Estep, and S. Tavener. A posteriori analysis and adaptive error control for operator decomposition solution of coupled semilinear elliptic systems. *International Journal for Numerical Methods in Engineering*, 94(9):826–849, 2013. ISSN 1097-0207. doi: 10.1002/nme.4482. URL <http://dx.doi.org/10.1002/nme.4482>.
- D. Chapelle, J.F. Gerbeau, J. Sainte-Marie, and I.E Vignon-Clementel. A poroelastic model valid in large strains with applications to perfusion in cardiac modeling. *Computational Mechanics*, 46(1):91–101, 2010.
- A.N. Cookson, J. Lee, C. Michler, R. Chabiniok, E. Hyde, D.A. Nordsletten, M. Sinclair, M. Siebes, and N.P. Smith. A novel porous mechanical framework for modelling the interaction between coronary perfusion and myocardial mechanics. *Journal of Biomechanics*, 45(5):850 – 855, 2012.
- O. Coussy. *Poromechanics*. John Wiley & Sons Inc, 2004.
- Daniele Antonio Di Pietro and Alexandre Ern. *Mathematical aspects of discontinuous Galerkin methods*, volume 69. Springer, 2011.
- H.C. Elman, D.J. Silvester, and A.J. Wathen. *Finite elements and fast iterative solvers: with applications in incompressible fluid dynamics*. Oxford University Press, USA, 2005.
- Xiaobing Feng and Yinnian He. Fully discrete finite element approximations of a polymer gel model. *SIAM Journal on Numerical Analysis*, 48(6):2186–2217, 2010.
- Massimiliano Ferronato, Nicola Castelletto, and Giuseppe Gambolati. A fully coupled 3-D mixed finite element model of Biot consolidation. *Journal of Computational Physics*, 229(12):4813–4830, 2010.
- F. Galbusera, H. Schmidt, J. Noailly, A. Malandrino, D. Lacroix, H.J. Wilke, and A. Shirazi-Adl. Comparison of four methods to simulate swelling in poroelastic finite element models of intervertebral discs. *Journal of the Mechanical Behavior of Biomedical Materials*, 4(7):1234 – 1241, 2011.
- P.A. Galie, R.L. Spilker, and J.P. Stegmann. A linear, biphasic model incorporating a Brinkman term to describe the mechanics of cell-seeded collagen hydrogels. *Annals of Biomedical Engineering*, 39:2767–2779, 2011.
- J.B Haga, H Osnes, and H.P Langtangen. On the causes of pressure oscillations in low-permeable and low-compressible porous media. *International Journal for Numerical and Analytical Methods in Geomechanics*, 36(12):1507–1522, 2012.
- M.H Holmes and V.C Mow. The nonlinear characteristics of soft gels and hydrated connective tissues in ultrafiltration. *Journal of Biomechanics*, 23(11):1145–1156, 1990.
- A-RA Khaled and K Vafai. The role of porous media in modeling flow and heat transfer in biological tissues. *International Journal of Heat and Mass Transfer*, 46(26):4989–5003, 2003.
- J Kim, HA Tchelepi, and R Juanes. Stability and convergence of sequential methods for coupled flow and geomechanics: Fixed-stress and fixed-strain splits. *Computer Methods in Applied Mechanics and Engineering*, 200(13):1591–1606, 2011.

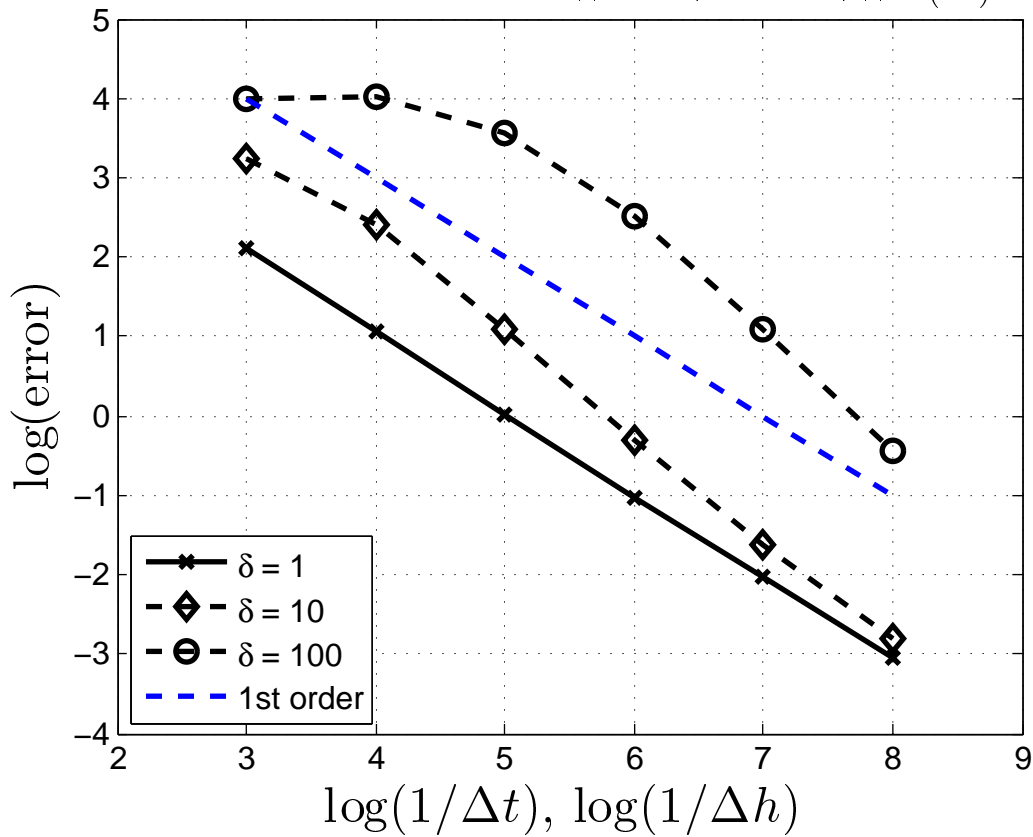
- B. S. Kirk, J. W. Peterson, R. H. Stogner, and G. F. Carey. `libMesh`: A C++ Library for Parallel Adaptive Mesh Refinement/Coarsening Simulations. *Engineering with Computers*, 22(3–4):237–254, 2006.
- P. Kowalczyk. Mechanical model of lung parenchyma as a two-phase porous medium. *Transport in Porous Media*, 11(3):281–295, 1993.
- Huanrong Li and Yukun Li. A discontinuous Galerkin finite element method for swelling model of polymer gels. *Journal of Mathematical Analysis and Applications*, 398(1):11–25, 2012.
- X.G. Li, H. Holst, J. Ho, and S. Kleiven. Three dimensional poroelastic simulation of brain edema: Initial studies on intracranial pressure. In *World Congress on Medical Physics and Biomedical Engineering*, pages 1478–1481. Springer, 2010.
- Konstantin Lipnikov. *Numerical methods for the Biot model in poroelasticity*. PhD thesis, University of Houston, 2002.
- R. Liu. *Discontinuous Galerkin finite element solution for poromechanics*. PhD thesis, The University of Texas at Austin, 2004.
- Steve A Maas, Benjamin J Ellis, Gerard A Ateshian, and Jeffrey A Weiss. FEBio: finite elements for biomechanics. *Journal of biomechanical engineering*, 134(1):1–10, 2012.
- V.C. Mow, S.C. Kuei, W.M. Lai, and C.G. Armstrong. Biphasic creep and stress relaxation of articular cartilage in compression: Theory and experiments. *Journal of Biomechanical Engineering*, 102:73–84, 1980.
- Márcio A Murad and Abimael FD Loula. On stability and convergence of finite element approximations of Biot’s consolidation problem. *International journal for numerical methods in engineering*, 37(4):645–667, 1994.
- Phillip Joseph Phillips and Mary F Wheeler. A coupling of mixed and continuous Galerkin finite element methods for poroelasticity i: the continuous in time case. *Computational Geosciences*, 11(2):131–144, 2007a.
- Phillip Joseph Phillips and Mary F Wheeler. A coupling of mixed and continuous Galerkin finite element methods for poroelasticity ii: the discrete-in-time case. *Computational Geosciences*, 11(2):145–158, 2007b.
- Phillip Joseph Phillips and Mary F Wheeler. A coupling of mixed and discontinuous Galerkin finite-element methods for poroelasticity. *Computational Geosciences*, 12(4):417–435, 2008.
- Phillip Joseph Phillips and Mary F Wheeler. Overcoming the problem of locking in linear elasticity and poroelasticity: an heuristic approach. *Computational Geosciences*, 13(1):5–12, 2009.
- R.E Showalter. Diffusion in poro-elastic media. *Journal of mathematical analysis and applications*, 251(1):310–340, 2000.
- Vidar Thomée. *Galerkin finite element methods for parabolic problems*, volume 25. Springer, 2006.

- R Verfürth. A posteriori error estimators for convection-diffusion equations. *Numerische Mathematik*, 80(4):641–663, 1998.
- Mary F Wheeler and Xiuli Gai. Iteratively coupled mixed and Galerkin finite element methods for poro-elasticity. *Numerical Methods for Partial Differential Equations*, 23(4):785–797, 2007.
- J.A. White and R.I. Borja. Stabilized low-order finite elements for coupled solid-deformation/fluid-diffusion and their application to fault zone transients. *Computer Methods in Applied Mechanics and Engineering*, 197(49-50):4353–4366, 2008.
- Joshua A White and Ronaldo I Borja. Block-preconditioned Newton–Krylov solvers for fully coupled flow and geomechanics. *Computational Geosciences*, 15(4):647–659, 2011.
- B. Wirth and I. Sobey. An axisymmetric and fully 3D poroelastic model for the evolution of hydrocephalus. *Mathematical Medicine and Biology*, 23(4):363–388, 2006.
- Son-Young Yi. A coupling of nonconforming and mixed finite element methods for Biot’s consolidation model. *Numerical Methods for Partial Differential Equations*, 2013.
- Alexander Ženíšek. The existence and uniqueness theorem in Biot’s consolidation theory. *Aplikace matematiky*, 29(3):194–211, 1984.

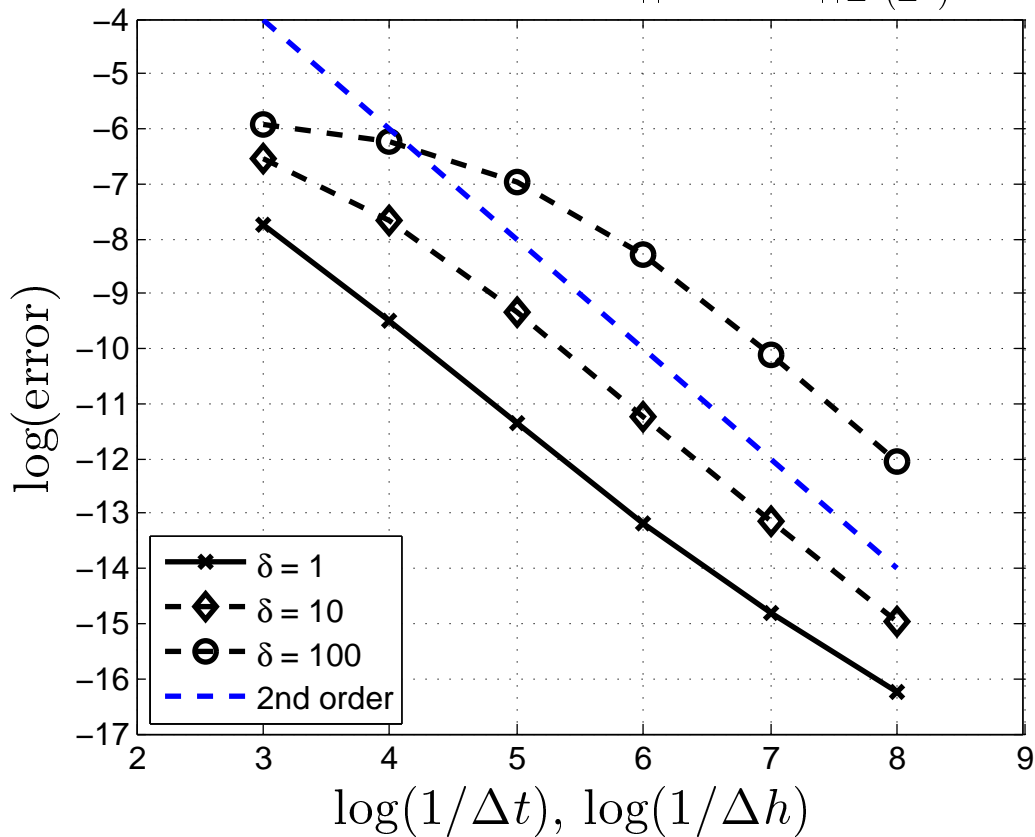
2D convergence of $\|\mathbf{u} - \mathbf{u}_h\|_{L^\infty(H^1)}$



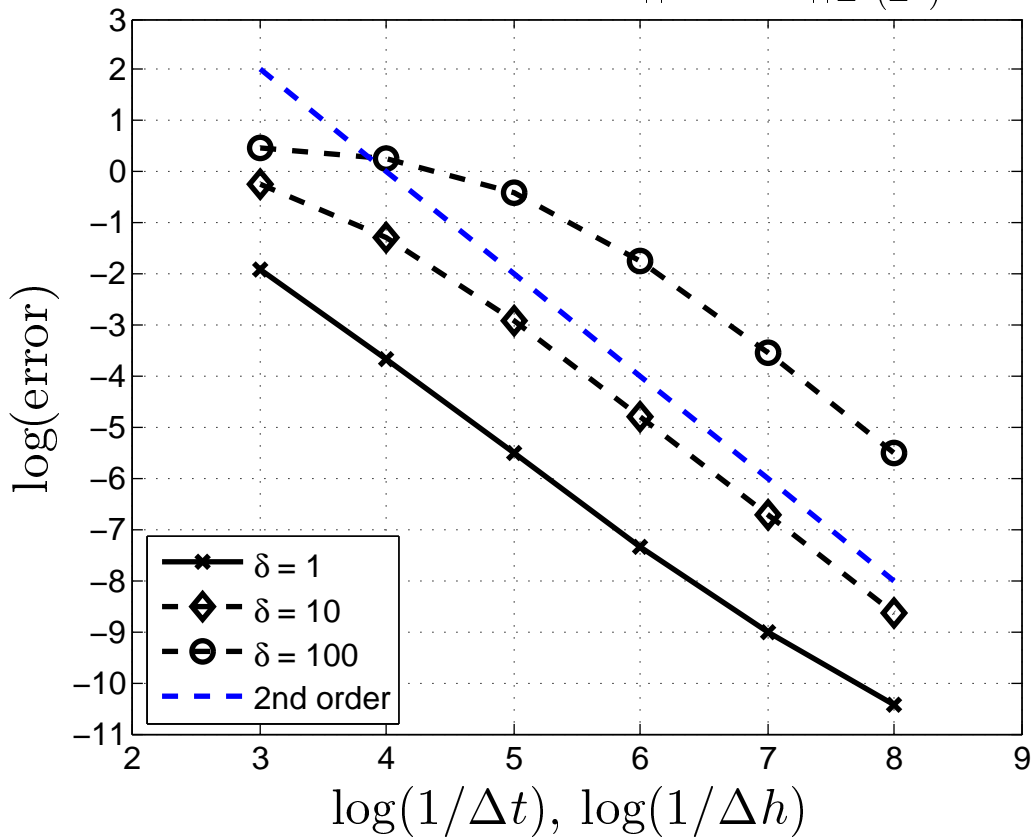
2D convergence of $||\nabla \cdot (\mathbf{z} - \mathbf{z}_h)||_{L^2(L^2)}$



2D convergence of $\|\mathbf{u} - \mathbf{u}_h\|_{L^2(L^2)}$



2D convergence of $\|\mathbf{z} - \mathbf{z}_h\|_{L^2(L^2)}$



2D convergence of $\|p - p_h\|_{L^\infty(L^2)}$

